Title: Mutations in enterobacterial common antigen biosynthesis restore outer membrane barrier function in *Escherichia coli tol-pal* mutants

Authors: Xiang'Er Jiang[a#], Wee Boon Tan[b#], Rahul Shrivastava[a#], Deborah Chwee San Seow[c], Swaine Lin Chen[d,e], Xue Li Guan[c], Shu-Sin Chng[a,b*]

Affiliations:

[a]Department of Chemistry, National University of Singapore, Singapore 117543.

[b]Singapore Center for Environmental Life Sciences Engineering, National University of Singapore (SCELSE-NUS), Singapore 117456.

[c]Lee Kong Chian School of Medicine, Nanyang Technological University, Singapore 636921.

[d]Yong Loo Lin School of Medicine, National University of Singapore, Singapore 119228.

[e]Genome Institute of Singapore, Agency for Science, Technology and Research (A*STAR), Singapore 138672.

[#]These authors contributed equally to the work.

*To whom correspondence should be addressed. E-mail: chmchngs@nus.edu.sg

Keywords: Tol-Pal complex, ECA, MPIase, lipid homeostasis, outer membrane barrier, vancomycin resistance

Summary

The outer membrane (OM) is an essential component of the Gram-negative bacterial envelope that protects cells against external threats. To maintain a functional OM, cells require distinct mechanisms to ensure balance of proteins and lipids in the membrane. Mutations in OM biogenesis and/or homeostasis pathways often result in permeability defects, but how molecular changes in the OM affect barrier function is unclear. Here, we seek potential mechanism(s) that can alleviate permeability defects in *Escherichia coli* cells lacking the Tol-Pal complex, which accumulate excess PLs in the OM. We identify mutations in enterobacterial common antigen (ECA) biosynthesis that re-establish OM barrier function against large hydrophilic molecules, yet did not restore lipid homeostasis. Furthermore, we demonstrate that build-up of biosynthetic intermediates, but not loss of ECA itself, contributes to the rescue. This suppression of OM phenotypes is unrelated to known effects that accumulation of ECA intermediates have on the cell wall. Finally, we reveal that an unusual diacylglycerol pyrophosphoryl-linked lipid species also accumulates in ECA mutants, and might play a role in the rescue phenotype. Our work provides insights into how OM barrier function can be restored independent of lipid homeostasis, and highlights previously unappreciated effects of ECA-related species in OM biology.

Introduction

Gram-negative bacteria are surrounded by a multilayered cell envelope consisting of the inner membrane (IM), the peptidoglycan layer, and the outer membrane (OM). This envelope structure, in particular the OM, plays an essential role in preventing toxic molecules from entering the cell, contributing to intrinsic resistance of Gram-negative bacteria against many antibiotics and detergents (Nikaido, 2003). The OM bilayer is asymmetric and has a unique lipid composition, comprising lipopolysaccharides (LPS) in the outer leaflet and phospholipids (PLs) in the inner leaflet. In the presence of divalent cations, LPS molecules in the outer leaflet pack together to form an impervious monolayer (Raetz & Whitfield, 2002); OM structure and lipid asymmetry are thus key determinants for its barrier function. Furthermore, the OM is essential for growth, highlighting the importance of understanding how it is established and maintained.

The biogenesis of the OM has been relatively well studied. Key components, including LPS, integral β-barrel proteins, and lipoproteins, are transported and assembled unidirectionally into the OM by the Lpt (Okuda et al., 2016), Bam (Hagan et al., 2011), and Lol machinery (Okuda & Tokuda, 2011), respectively. Recently, several systems, including the OmpC-Mla system and the Tol-Pal complex, have been implicated in PL transport between the IM and the OM (Shrivastava et al., 2017; Ekiert et al., 2017; Ercan et al., 2018; Thong et al., 2016; Hughes et al., 2019). However, much of bulk PL transport between the two membranes, which occurs in both directions (Donohue-Rolfe & Schaechter, 1980; Jones & Osborn, 1977; Langley et al., 1982), is still largely unknown (Shrivastava & Chng, 2019). Nonetheless, an intricate balance between these different OM biogenesis pathways needs to be maintained at all times to ensure a stable OM. Such homeostasis

59 of OM components is critical for proper barrier function; yet, we do not fully understand the exact
60 molecular mechanisms of how changes in the OM can translate to permeability defects. In many
61 cases, mutations in OM biogenesis (e.g. *lptD4213, degP, bamB, tol-pal*) result in compromised
62 OM barrier function against both hydrophobic molecules, such as detergents, and even large
63 hydrophilic antibiotics, including vancomycin. One common problem with the OM in these
64 mutants appears to be perturbations in the lipid asymmetry. This give rises to PL bilayer patches
65 that would allow easier diffusive passage of hydrophobic compounds, but not hydrophilic ones.
66 How large hydrophilic drugs like vancomycin cross the OM in mutants with defective OM
67 biogenesis remains elusive.

68 The Tol-Pal complex is a conserved multi-protein system that forms a trans-envelope bridge
69 across the cell envelope in Gram-negative bacteria, and has been known to be generally important
70 for OM stability and integrity (Lloubes et al., 2001; Sturgis, 2001; Cascales et al., 2000). It
71 comprises two sub-complexes: TolQRA in the IM and TolB-Pal at the OM. We recently
72 demonstrated that the Tol-Pal complex is involved in the maintenance of OM lipid homeostasis in
73 *Escherichia coli* (Shrivastava et al., 2017). Cells lacking the intact complex accumulate excess PLs
74 in the OM, likely due to defects in retrograde (OM-to-IM) PL transport. This increase in PL content
75 may contribute to many known OM permeability/stability phenotypes in *tol-pal* mutants, including
76 hypersensitivity to antibiotics and detergents, leakage of periplasmic content, and OM
77 hypervesiculation (Lloubes et al., 2001; Bernadac et al., 1998). The Tol-Pal complex also plays a
78 key role in cell division; mutant strains lacking functional Tol-Pal exhibits division defects under
79 extreme osmolarity due to incomplete septal cell wall separation and/or improper OM invagination

80 (Gerding et al., 2007; Yakhnina & Bernhardt, 2020). Its role in cell division appears to be
81 independent of its function in OM lipid homeostasis (Yakhnina & Bernhardt, 2020).

82 Lipid dyshomeostasis in cells lacking the Tol-Pal complex affects OM barrier function in a
83 way that allows entry of both hydrophobic molecules and large hydrophilic antibiotics. To gain
84 insight(s) into OM lipid homeostasis and how it possibly affects OM function, we asked whether
85 cells lacking the Tol-Pal complex could restore OM barrier function by compensatory mutations
86 in other pathways. We found that disruption in the biosynthesis of enterobacterial common antigen
87 (ECA), a cell surface polysaccharide in the Enterobacteriaceae family (Kuhn et al., 1988), rescues
88 OM permeability defects in *tol-pal* mutants, especially against large hydrophilic molecules
89 including antibiotics and periplasmic proteins. Interestingly, in these suppressor mutants, OM lipid
90 homeostasis is still defective even though barrier function is restored. We demonstrated that the
91 rescue requires the accumulation of ECA intermediates, yet is independent of known effects of
92 such build-up on cell wall integrity. Finally, we detected unusual ECA-related lipids in these cells,
93 raising the possibility that they might play a role in restoring OM phenotypes. Our work reveals
94 that the OM barrier, specifically against large hydrophilics, can somehow be re-established even
95 during lipid dyshomeostasis, highlighting the complex and dynamic nature of bacterial OM
96 permeability.

97 **Results**

98

99 **Loss-of-function mutations in ECA biosynthesis rescue OM permeability defects in *tol-pal***

100 **mutants**

101 Cells lacking the Tol-Pal complex have compromised OM integrity due to the accumulation

102 of excess PLs (Shrivastava et al., 2017). To gain insight(s) into this phenomenon, we sought to

103 isolate genetic suppressor mutations that could restore OM barrier function in a Δ*tol-pal* mutant.

104 We selected for suppressors that rescue sensitivity to vancomycin, the large cell wall-targeting

105 antibiotic that cannot penetrate an intact and functional OM (Krishnamoorthy et al., 2016). Cells

106 have no intrinsic mechanism to alter cell wall structure to give rise to resistance against

107 vancomycin; consistently, suppressor colonies appeared at a low frequency of ~1 x 10^{-9}. We

108 obtained 36 individual suppressor strains, all of which exhibited stable resistance phenotypes

109 against vancomycin similar to a wild-type (WT) strain. We further examined the susceptibilities of

110 these strains against other commonly used antibiotics, including rifampicin and erythromycin. An

111 intact OM also impedes the entry of rifampicin and erythromycin but less effectively than against

112 vancomycin (Krishnamoorthy et al., 2016). Eight of the suppressors exhibited near wild-type level

113 resistance against vancomycin and erythromycin (Fig. S1A), thus appearing to have restored OM

114 barrier function. Consistent with this, many of these strains release less periplasmic RNase I into

115 the media during growth when compared to the parent Δ*tol-pal* mutant (Fig. S1B). We sequenced

116 the genomes of the parent strain and all eight suppressors. Each suppressor strain contains multiple

117 mutations relative to the parent Δ*tol-pal* mutant (Table S1). Many strains contain mutations in

118 either *pgm* or *mdoH* (*opgH*), which have already been implicated in conferring vancomycin
119 resistance, especially at low temperature (Stokes et al., 2016). Interestingly, all of these strains
120 have mutations in genes involved in the biosynthesis of ECA (*wecB*, *wecC*, or *wecF*), so we
121 decided to further investigate this genetic interaction.

122 Six strains contain mutations in *wecC*, which encodes a dehydrogenase enzyme in the ECA
123 synthesis pathway (Kuhn et al., 1988; Meier-Dieter et al., 1990). A 6-bp in-frame insertion in *wecC*,
124 termed *wecC**, is common to four of these strains, suggesting that this allele may be important for
125 restoring OM barrier function in the Δ*tol-pal* mutant. To validate this, we re-constructed the *wecC** 126 mutation in the native locus using a negative selection technique (Khetrapal et al., 2015) and
127 confirmed that this allele alone is able to partially rescue antibiotic sensitivity (Figs. 1A, S2A) and
128 periplasmic leakiness, albeit to different extents in Δ*tolQ*, Δ*tolA*, and Δ*tolB* strains (Fig. S2B).
129 These partial rescue phenotypes are consistent with the idea that *pgm* and/or *mdoH* (*opgH*)
130 mutations found in the original suppressor strains also contribute to restoring OM function (Stokes
131 et al., 2016).

132 The *wecC** mutation results in the insertion of two amino acids (Pro and Gly) five residues
133 away from the predicted active site Cys in the full-length protein, suggesting that WecC function
134 may be disrupted. Consistent with this, we did not detect any ECA in strains containing this *wecC** 135 allele (Fig. 1C). Furthermore, we showed that deletion of *wecC* also partially restores vancomycin
136 resistance in *tol-pal* strains (Figs. 1B and C). We isolated *wecB* and *wecF* mutations in two of the
137 sequenced suppressor strains (Table S1); we therefore constructed Δ*wecB* and Δ*wecF* mutants to
138 test their rescue phenotypes. Both null mutations partially rescue vancomycin sensitivity in the

139 Δ*tolA* strain (Fig. 1D). Finally, we showed that the Δ*wecC* mutation does not suppress vancomycin
140 sensitivity in strains with other OM defects (*lptD4213* and *bepA*) (Fig. S3). We conclude that loss-
141 of-function mutations in ECA biosynthesis likely restore the OM barrier function specifically in
142 strains lacking the Tol-Pal complex.
143

144 **Mutations in ECA biosynthesis restore OM barrier function in *tol-pal* strains independent of**
145 **Rcs phosphorelay pathway and/or capsular polysaccharide biosynthesis**

146 Mutations in the ECA pathway are known to trigger the Rcs phosphorelay stress response
147 (Castelli & Vescovi, 2011). *tol-pal* mutations also strongly activate the Rcs signaling cascade
148 (Clavel et al., 1996). Consequently, combined *tol-pal*/ECA mutant colonies exhibit strongly
149 mucoidal phenotypes, presumably due to the over-production of capsular polysaccharides (colanic
150 acids), which is regulated by the Rcs pathway (Stout & Gottesman, 1990; Trisler & Gottesman,
151 1984). We therefore considered whether hyperactivation of the Rcs stress response or up-regulation
152 of colanic acid biosynthesis contributed to the suppression of vancomycin sensitivity by ECA
153 mutations in the *tol-pal* strains. To test this idea, we examined vancomycin sensitivity in *rcsC*
154 (encoding the histidine sensor kinase of the Rcs pathway) (Stout & Gottesman, 1990) or *wcaJ*
155 (encoding the glycosyl transferase that initiates colanic acid biosynthesis) (Stevenson et al., 1996)
156 mutants. Deleting *rcsC* or *wcaJ* did not prevent the Δ*wecC* mutation from suppressing vancomycin
157 sensitivity in the Δ*tolA* strain; instead, the Δ*rcsC* Δ*tolA* Δ*wecC* and Δ*wcaJ* Δ*tolA* Δ*wecC* mutants
158 display full resistance against vancomycin, similar to WT cells (Fig. 2A). The mechanism by which
159 the Δ*wecC* mutation suppresses vancomycin sensitivity in *tol-pal* strains is therefore independent

160 of the Rcs phosphorelay and/or colanic acid synthesis.

161 To further demonstrate that the OM barrier function was indeed restored, we showed that
162 Δ*wecC* partially rescues rifampicin and erythromycin sensitivity (Fig. S4) and fully restores
163 bacitracin resistance in the Δ*wcaJ* Δ*tolA* strain (Fig. 2B). Furthermore, we demonstrated that a
164 fluorescent analog of vancomycin (BODIPY FL vancomycin) could only penetrate the OM and
165 label peptidoglycan in the Δ*wcaJ* Δ*tolA* strain, but not the Δ*wcaJ* Δ*tolA* Δ*wecC* triple mutant (Fig.
166 2C). The Δ*wcaJ* Δ*tolA* Δ*wecC* strain also exhibited reduced periplasmic leakiness compared to the
167 Δ*wcaJ* Δ*tolA* mutant (Fig. 2D). Rifampicin (MW ~823) and erythromycin (MW ~734) are much
168 smaller than vancomycin (MW ~1449) and bacitracin (MW ~1423). We conclude that the Δ*wecC*
169 mutation restores OM barrier function in the *tol-pal* strains lacking colanic acid synthesis,
170 especially against the passage of larger hydrophilic molecules, including vancomycin, bacitracin,
171 and periplasmic proteins (e.g. RNase I).

172 We have observed that the Δ*wecC* mutation rescues vancomycin sensitivity in the Δ*tolA* strain;
173 however, we noted that different transductants display varying extents of suppression (Fig. S5).
174 We found that removing RcsC or WcaJ greatly improved the consistency of suppression of the
175 Δ*tolA* phenotype by the Δ*wecC* mutation. This suggests that the initial variability in suppression
176 could be due to varying mucoidal phenotypes, possibly because of stochasticity of colanic acid
177 overproduction. This might additionally explain why the *wecC** and Δ*wecC* mutations also showed
178 different levels of rescue in Δ*tolQ*, Δ*tolA*, and Δ*tolB* strains that still produce colanic acids (Figs.
179 1, S2). To eliminate this inconsistency, we used strains deleted of *wcaJ* for the rest of this study.

180

181 **Mutations in ECA biosynthesis rescue OM barrier function without restoring lipid**
182 **homeostasis in *tol-pal* mutants**

183 Cells lacking the Tol-Pal complex accumulate excess PLs (relative to LPS) in the OM due to
184 defective retrograde PL transport (Shrivastava et al., 2017). Since mutations in the ECA
185 biosynthetic pathway rescue OM defects in *tol-pal* mutants (Fig. 1), we hypothesized that OM
186 lipid homeostasis is restored in these strains. To test this idea, we examined steady state OM lipid
187 compositions in Δ*wcaJ* Δ*tolA* Δ*wecC* mutant cells by measuring the distribution of [^{32}P]-
188 phosphate-labelled PLs between the IM and the OM, and also determining the ratio of PLs to LPS
189 (also labelled with [^{32}P]) in the OM. Consistent with our previous findings, the Δ*tolA* mutant
190 contained more PLs in the OM than WT cells (here in the Δ*wcaJ* background). Specifically, cells
191 lacking TolA accumulate ~1.7-fold excess PLs in the OM (relative to the IM) (Fig. 3A).
192 Furthermore, these cells have ~1.4-fold higher PL/LPS ratio in the OM (Fig. 3B). To our surprise,
193 deleting *wecC* in the Δ*tolA* strain neither re-established intermembrane PL distribution (Fig. 3A),
194 nor restored the OM PL/LPS ratio back to wild-type (Fig. 3B). Consistently, the Δ*tolA* and Δ*tolA*
195 Δ*wecC* strains produced similarly high levels of OM vesicles (Fig. 3C), a phenotype in part
196 attributed to excess PLs in the OM (Shrivastava et al., 2017). Even though the OM barrier function
197 (restriction of vancomycin/bacitracin entry and periplasmic RNase I release) has largely been
198 restored (Fig. 2), we conclude that mutations in ECA biosynthesis do not restore OM lipid
199 homeostasis in cells lacking the Tol-Pal complex.

200

201 **Accumulation of ECA intermediates along the biosynthetic pathway is critical for rescue of**

202 **OM barrier function in *tol-pal* strains**

203 The initial steps of ECA biosynthesis involve successive addition of three sugar moieties (*N*-
204 acetyl-D-glucosamine (GlcNAc), *N*-acetyl-D-mannosaminuronic acid (ManNAcA), and 4-
205 acetamido-4,6-dideoxy-D-galactose (Fuc4NAc)) to the undecaprenyl phosphate (und-P) lipid
206 carrier to form Lipid III^{ECA} (Kuhn et al., 1988; Rahman et al., 2001). After its synthesis at the inner
207 leaflet of the IM, Lipid III^{ECA} is flipped across the membrane by WzxE (Rick et al., 2003). This
208 trisaccharide repeating unit is then polymerized by WzyE to form the complete ECA polymer,
209 whose polysaccharide chain length is regulated by WzzE (Kajimura et al., 2005; Barr et al., 1999).
210 The whole ECA polymer, which is now carried on undecaprenyl pyrophosphate (und-PP), is finally
211 transferred to form a phosphatidyl-linked species (ECA_{PG}) before being transported to the OM
212 (Kuhn et al., 1983; Rinno et al., 1980; Acker et al., 1986) (Fig. 4A). The enzymes mediating the
213 last two steps are not known. Of note, two other minor forms of ECA are produced, including a
214 soluble cyclic form in the periplasm (ECA_{CYC}) and one that is found attached to LPS (ECA_{LPS})
215 (Kuhn et al., 1988). The production of these two ECA forms is dependent on WzzE and the LPS
216 O-antigen ligase WaaL, respectively (Kajimura et al., 2005; Schmidt et al., 1976; Mitchell et al.,
217 2018).

218 We have shown that loss-of-function mutations in *wecB*, *wecC*, and *wecF* rescue vancomycin
219 sensitivity in *tol-pal* mutants (Fig. 1). Mutations in ECA biosynthesis result in both the loss of
220 surface ECA and the build-up of intermediates (Lipid $I/II/III^{ECA}$) along the pathway (Fig. 4A). To
221 test whether ECA loss is important, we mutated *wecA*, which encodes the enzyme that catalyzes
222 the first committed step in ECA biosynthesis. Interestingly, we found that the Δ*tolA* Δ*wecA* mutant

223 (in the Δ*wcaJ* background) is equally sensitive to vancomycin as the Δ*tolA* mutant (Fig. 4B),
224 suggesting that accumulation of intermediates along the ECA pathway, but not the loss of any form
225 of ECA (ECA_{PG}, ECA_{LPS}, or ECA_{CYC}), is responsible for the suppression. Consistent with this idea,
226 removing other ECA biosynthetic enzymes that result in accumulation of intermediates (Lipid I^{ECA}
227 in Δ*wecG*, or Lipid II^{ECA} in Δ*wecE*) fully rescues vancomycin sensitivity in the Δ*tolA* mutant (Fig.
228 4B). Expressing the deleted *wec* genes *in trans* reversed this effect (Fig. S6A). Importantly, rescue
229 of vancomycin sensitivity in these strains was completely abolished when *wecA* was subsequently
230 deleted (Fig. 4C). Likewise, expressing *wecA* in these strains *in trans* re-establish the rescue (Fig.
231 S6B). We conclude that the build-up of Lipid I^{ECA} or Lipid II^{ECA} intermediates can somehow
232 restore OM barrier function in the absence of the Tol-Pal complex.

233 We next tried to test whether mutations in later steps of ECA biosynthesis also suppress *tol-*
234 *pal* phenotypes. We found that removing WzxE, the Lipid III^{ECA} flippase, does not rescue
235 vancomycin sensitivity in the Δ*tolA* strain (Fig. S7A). However, the Δ*wzxE* mutant still produces
236 full length ECA (Fig. S7B), presumably because the O-antigen flippase WzxB can also transport
237 Lipid III^{ECA} (Rick et al., 2003), thus preventing its accumulation. Nonetheless, it has been reported
238 that completely blocking translocation across the IM or subsequent polymerization of Lipid III^{ECA}
239 causes toxicity in cells (Rick et al., 2003; Kajimura et al., 2005; Baba et al., 2006); removing both
240 flippases (WzxE and WzxB) or the polymerase (WzyE) is lethal (Figs. S7C, D), precluding further
241 analysis. We therefore turned our attention to WzzE. Remarkably, deletion of *wzzE* partially
242 rescues vancomycin sensitivity in the Δ*tolA* mutant, and this phenotype is dependent on the
243 presence of WecA (Fig. 5A). Cells lacking WzzE are known to lose modality in the ECA polymer,

giving rise to a more random distribution of chain lengths (Barr et al. 1999). We validated this observation; there are relatively higher levels of shorter chain ECA, presumably including Lipid III^{ECA} precursors, in the Δ*wzzE* mutant (Fig. 5B). Taken together, our results suggest that build-up of short-chain or Lipid III^{ECA} intermediates can also possibly rescue OM defects in cells lacking the Tol-Pal complex.

It has previously been reported that the terminal GlcNAc moiety attached to the *E. coli* K-12 LPS core oligosaccharide is derived from und-PP-GlcNAc (i.e. Lipid I^{ECA}) via the action of WaaL (Feldman et al., 1999; Ruan et al., 2018). Since WaaL accepts different und-PP-linked substrates, it may be possible that corresponding modifications of LPS can occur in strains accumulating Lipid II/III^{ECA}; these modified LPS might contribute to restored OM barrier function in the *tol-pal* mutants. To test this idea, we checked if the rescue of vancomycin sensitivity in the Δ*tolA* Δ*wecC* strain is dependent on WaaL. We found that deleting *waaL* did not confer vancomycin sensitivity to the Δ*tolA* Δ*wecC* mutant (Fig. S8), suggesting that the suppression of OM permeability defects is not due to WaaL-dependent LPS modifications.

Suppression of OM permeability defects in *tol-pal* strains via accumulation of ECA intermediates is independent of und-P sequestration or σ^E and Cpx stress response pathways

Recently, it has been reported that the build-up of ECA "dead-end" intermediates can lead to sequestration of und-P, the common precursor for many sugar polymers in the cell envelope including peptidoglycan; this gives rise to shape defects such as filamentation and swelling (Jorgenson et al., 2016; Campos et al., 2018). In our strains that lack colanic acids, we also observe

265 similar shape defects. We measured primarily larger cell width in the Δ*wecC* mutant, which were
266 exacerbated in the Δ*tolA* background (Figs. S9A, B). The morphological changes observed in the
267 Δ*tolA* Δ*wecC* strain are thus a combination of defects due to the loss of Tol-Pal function (Rassam
268 et al., 2018), and und-P sequestration caused by accumulation of ECA intermediates (Jorgenson et
269 al., 2016). To test whether und-P sequestration contributes to the rescue of vancomycin sensitivity
270 in the Δ*tolA* Δ*wecC* strain, we examined if overexpression of MurA, which can alleviate und-P
271 sequestration effects by directing the lipid carrier towards peptidoglycan biosynthesis (Jorgenson
272 et al., 2016), could reverse the phenotypes. As expected, MurA overexpression was able to fully
273 and partially revert the cell morphological defects in Δ*wecC* and Δ*tolA* Δ*wecC* strains, respectively
274 (Figs. S9A, B, D). However, doing so did not alter vancomycin resistance in the Δ*tolA* Δ*wecC*
275 mutant (Figs. S9C, D). Similarly, vancomycin sensitivity was not restored when overexpressing
276 UppS, which is expected to increase the und-P pool (Jorgenson et al., 2016). These data indicate
277 that the effect of accumulation of ECA intermediates in restoring OM barrier function in *tol-pal*
278 mutants is independent of und-P sequestration.

279 Accumulation of ECA intermediates, specifically Lipid II^{ECA}, is also known to stimulate the
280 σ^E and Cpx stress response pathways (Danese et al., 1998). However, we did not observe
281 significant induction or increased stimulation of σ^E when ECA intermediates were accumulated in
282 WT or Δ*tolA* strains, respectively (Fig. S10A). Removing the Cpx pathway also did not affect
283 vancomycin resistance in the Δ*tolA* Δ*wzzE* strain (Fig. S10B). We conclude that both σ^E and Cpx
284 stress responses are also not involved in the ability of accumulated ECA intermediates to restore
285 the OM barrier function in *tol-pal* mutants.

286

287 **Diacylglycerol pyrophosphoryl-linked species accumulate in ECA biosynthesis mutants in**

288 **addition to undecaprenyl pyrophosphoryl-linked intermediates**

289 We have shown that accumulation of ECA intermediates rescues vancomycin sensitivity in

290 strains lacking the Tol-Pal complex. However, und-PP-linked intermediates (Lipid I/II/III^{ECA}) may

291 not be the only species accumulated in ECA biosynthesis mutants. In a *Salmonella* Typhimurium

292 Δ*rmlA* mutant, which accumulates Lipid II^{ECA}, a novel diacylglycerol pyrophosphoryl (DAG-PP)-

293 linked species containing the first two sugars of ECA (GlcNAc and ManNAcA) was detected at

294 comparable levels (Rick et al., 1998). We therefore sought to determine whether DAG-PP-linked

295 adducts could also be found in our *E. coli* ECA mutants. Using high resolution mass spectrometry

296 (MS), we analyzed lipids extracted from cells lacking WecG; as expected, we saw accumulation

297 of the und-PP-GlcNAc or Lipid I^{ECA} (m/z 1128.7026) intermediate (Fig. 6). Furthermore, we

298 demonstrated that DAG-PP-GlcNAc species are indeed present in these cells, but not in WT (Figs.

299 7A, B). Specifically, we detected peaks with m/z values corresponding to DAG-PP-GlcNAc

300 species with various fatty acid compositions in the DAG moiety, namely 32:1 (m/z 928.4927), 34:1

301 (m/z 956.5243), 34:2 (m/z 954.5076), and 36:2 (m/z 982.5391); these are in fact the major DAGs

302 found in native PLs in *E. coli* (Oursel et al., 2018). Chemical structures of the 32:1 and 34:1 species

303 were assigned and elucidated based on fragmentation patterns in MS/MS (Fig. 8). Furthermore,

304 we showed that the same species were specifically found in the IM but not the OM of the Δ*wecG*

305 mutant, as well as the Δ*wecC* strain (Fig. 7C). It is worth noting that DAG-PP has one extra

306 phosphate moiety and is therefore structurally distinct from phosphatidic acid (i.e. diacylglycerol

307 monophosphate or DAG-P), the final lipid carrier of ECA; instead, the DAG-PP-GlcNAc and
308 DAG-PP-GlcNAc-ManNAc species (Rick et al., 1998) have been suggested as structural
309 precursors to the MPIase glycolipid (Nishiyama et al., 2012; Sawasato et al., 2019a), which is
310 required for protein integration and translocation at the IM. How these DAG-PP-linked species are
311 generated is not fully understood, but their existence highlights the need to consider possible
312 effects of these unusual lipids in our ECA biosynthesis mutants, especially in the context of
313 rescuing OM barrier function in *tol-pal* strains.

314 **Discussion**

315 In this study, we have identified suppressor mutations that can rescue OM permeability defects
316 in cells lacking the Tol-Pal complex, which are known to contain excess PLs in their OM
317 (Shrivastava et al., 2017; Masilamani et al., 2018). Mutations in ECA biosynthesis restore OM
318 barrier function, thus blocking entry of large antibiotics and reducing periplasmic leakiness, in *tol-*
319 *pal* mutant strains (Figs. 1, 2); however, lipid homeostasis was not restored in these strains (Fig.
320 3). We have demonstrated that these rescue phenotypes are due to the accumulation of intermediate
321 species along the ECA pathway (Figs. 4, 5). Interestingly, aside from the und-PP-linked ECA
322 intermediates (Fig. 6), DAG-PP-linked species have also been observed (Figs. 7, 8). How the
323 presence of these ECA-related species could result in the restoration of OM barrier function
324 requires further investigation.

325 The role of ECA in the enterobacterial cell envelope is not known. Strains that do not make
326 ECA are more sensitive to bile salts and produce more OMVs (Ramos-Morales et al., 2003;
327 McMahon et al., 2012). Loss of cyclic ECA has also been reported to reverse OM barrier defects
328 in strains lacking YhdP, a protein of unknown function (Mitchell et al., 2018). These observations
329 suggest that ECA has roles related to the OM. However, we have shown that loss of any form of
330 ECA (ECA_{PG}/ECA_{LPS}/ECA_{CYC}) does not contribute to the restoration of OM barrier function in
331 cells lacking the Tol-Pal complex; instead, the build-up of ECA biosynthetic intermediates is
332 necessary for this rescue. Interestingly, accumulation of und-PP-linked intermediates (in the ECA,
333 O-antigen, and colanic acid pathways) can lead to sequestration of und-P (Jorgenson et al., 2016;
334 Jorgenson & Young, 2016), the common lipid carrier also used for peptidoglycan precursors. This

335 can give rise to morphological changes due to a weakened cell wall (Figs. S9A, B). Overexpression
336 of MurA to alleviate und-P sequestration effects reduced the extent of morphological defects but
337 could not reverse the suppression of *tol-pal* phenotypes (Fig. S9). Intuitively, weakening the cell
338 wall via und-P sequestration is unlikely to contribute to vancomycin and bacitracin resistance. We
339 therefore believe that restoration of OM phenotypes by ECA intermediates in cells lacking the Tol-
340 Pal complex is independent of und-P sequestration. Furthermore, the rescue mechanism does not
341 appear to involve the major cell envelope stress responses, including Rcs, Cpx, and σ^E pathways
342 (Figs. 2, S10).

343 One possible mechanism where accumulation of und-PP-linked ECA intermediates could
344 affect the physical properties of the OM is via LPS modification. The structure of LPS could affect
345 mechanical strength and barrier function of the OM (Rojas et al., 2018). In wild-type cells, the full
346 length ECA polymer can be transferred onto LPS core oligosaccharides by WaaL to form ECA_{LPS}
347 (Schmidt et al., 1976). However, since deletion of either *wecA* (does not restore OM barrier
348 function) or other *wec* genes (restore OM barrier function) would result in the loss of full length
349 ECA_{LPS}, we ruled out the role of ECA_{LPS} in rescuing the OM permeability defect. It has been
350 reported that the GlcNAc moiety from und-PP-GlcNAc (Lipid I^{ECA}) can itself be transferred onto
351 LPS in a WaaL-dependent manner (Feldman et al., 1999; Ruan et al., 2018). We reasoned it is
352 likely that the incomplete sugar subunits on Lipid II/III^{ECA} could also be ligated onto LPS,
353 therefore affecting the physical properties of the OM via LPS modification. However, we showed
354 that deletion of *waaL* in strains that accumulate ECA intermediates did not reverse the suppression

355 of OM permeability defects in the *tol-pal* mutant (Fig. S8). Therefore, the rescue of OM defects
356 by ECA mutations in *tol-pal* strains is unlikely due to WaaL-dependent LPS modifications.

357 While und-PP-linked intermediates are expected to be accumulated in ECA mutants, we and
358 others have also observed the corresponding DAG-PP-linked species (Rick et al., 1998).
359 Specifically, DAG-PP-GlcNAc and DAG-PP-GlcNAc-ManNAc species have been detected in
360 strains that accumulate und-PP-GlcNAc (Lipid I^{ECA}) (Fig. 7) and und-PP-GlcNAc-ManNAc (Lipid
361 II^{ECA}) (Rick et al., 1998), respectively. Intriguingly, these unusual DAG-PP-linked species have
362 been suggested to be precursors for the membrane protein integrase (MPIase) glycolipid, which in
363 fact has a polymer of 9-11 trisaccharide units (identical to the ECA sugars) linked to the DAG-PP
364 carrier (Nishiyama et al., 2012). It has been shown that MPIase is important for driving integration
365 of membrane proteins into the IM, and also Sec-dependent translocation of periplasmic and OM
366 proteins across the membrane (Nishiyama et al., 2012; Sawasato et al., 2019b). MPIase
367 biosynthesis has been shown to require the activity of CdsA (Sawasato et al., 2019a), the CDP-
368 diacylglycerol synthase critical for PL synthesis; however, despite the identical trisaccharide units,
369 this process appears to be independent of the ECA pathway (Kamemoto et al., 2019).
370 Consequently, it is not clear how and why DAG-PP-linked species, the presumed precursors to
371 MPIase, would accumulate in ECA biosynthesis mutants. Regardless, we need to consider possible
372 effects of these unusual lipids. We therefore speculate that these DAG-PP-linked species detected
373 in our suppressor strains might somehow modulate the essential membrane protein integration or
374 protein translocation functions of MPIase, possibly affecting a broad spectrum of pathways, and
375 thus indirectly resulting in restored OM barrier function even in the event of lipid dyshomeostasis.

376 The interesting connections between ECA, DAG-PP-linked species, and MPIase, remain to be
377 clarified.

378 Cells lacking the Tol-Pal complex exhibit both cell division and OM stability/permeability
379 defects. The cell division defect, which is more apparent under extreme osmolarity conditions, is
380 thought to be a problem in OM invagination (Gerding et al., 2007) but recently shown to be also
381 related to incomplete septal cell wall separation (Yakhnina & Bernhardt, 2020). The OM defects
382 are largely independent of cell division (Yakhnina & Bernhardt, 2020), and likely due to lipid
383 dyshomeostasis, where excess PLs accumulate in the OM (Shrivastava et al., 2017). While excess
384 PLs in the OM necessarily affect lipid asymmetry (Shrivastava et al., 2017) and result in PL bilayer
385 patches that can allow diffusion of hydrophobic molecules, it is unclear how that would increase
386 permeation of large hydrophilic molecules, such as vancomycin, bacitracin, and RNase I, across
387 the OM. One possibility is that having more PLs in the OM alters physical properties such as
388 membrane tension and rigidity. These effects could in turn result in the appearance of transient
389 "cracks" in the bilayer, which have been suggested to allow the passage of large hydrophilic
390 compounds (Nikaido, 2005; Ruiz et al., 2006). Vancomycin can also cross the OM via the lumen
391 of large porins, if unplugged (Krishnamoorthy et al., 2016). Therefore, another possibility is that
392 the changes in lipid composition in the OM of cells lacking the Tol-Pal complex may affect the
393 structure and function of specific large OM porins, causing them to become leaky. How the
394 accumulation of und-PP-linked ECA intermediates and/or DAG-PP-linked species restores OM
395 barrier function against large hydrophilic molecules remains unclear; however, these species might
396 affect other yet-to-be-identified pathways (e.g. MPIase function), possibly indirectly modifying

397 OM physical properties or porin function. The unappreciated roles of ECA-related species in OM

398 biology should be thoroughly investigated.

399 **Experimental Procedures**

400

401 **Strains and growth conditions.** All the strains used in this study are listed in Table S2.
402 *Escherichia coli* strain MC4100 [F^- *araD139* Δ*(argF-lac) U169 rpsL150 relA1 flbB5301 ptsF25*
403 *deoC1 ptsF25 thi*] (Casadaban, 1976) was used as the wild-type (WT) strain for most of the
404 experiments. NR754, an $araD^+$ revertant of MC4100 (Ruiz et al., 2008), was used as the WT strain
405 for experiments involving depletion of *wzxE* or *wzyE* from the arabinose-inducible promoter
406 (P_{BAD}). Gene deletion mutants were constructed using recombineering (Baba et al., 2006; Datsenko
407 et al., 2000) or obtained from the Keio collection (Baba et al, 2006). Whenever needed, the
408 antibiotic resistance cassettes were flipped out as described (Baba et al., 2006; Datsenko et al.,
409 2000). Gene deletion cassettes were transduced into relevant genetic background strains via P1
410 transduction (Silhavy et al., 1984). The unmarked and chromosomal *wecC** allele was constructed
411 using a negative selection technique (Khetrapal et al., 2015). Luria-Bertani (LB) broth (1%
412 tryptone and 0.5% yeast extract, supplemented with 1% NaCl) and agar were prepared as
413 previously described (Silhavy et al., 1984). When appropriate, kanamycin (kan; 25 μg ml^{-1}),
414 chloramphenicol (cm; 30 μg ml^{-1}), ampicillin (amp; 200 μg ml^{-1}) and spectinomycin (spec; 50 μg
415 ml^{-1}) were added.

416

417 **Plasmid construction.** Plasmids used in this study are listed in Table S3. Desired genes were
418 amplified from MC4100 chromosomal DNA using the indicated primers (sequences in Table S4).
419 Amplified products were digested with indicated restriction enzymes (New England Biolabs),

420 which were also used to digest the carrying vector. After ligation, recombinant plasmids were
421 transformed into competent NovaBlue (Novagen) cells and selected on LB plates containing
422 appropriate antibiotics. DNA sequencing (Axil Scientific, Singapore) was used to verify the
423 sequence of the cloned gene.
424
425 **Generation of suppressor mutations and genome sequencing.** To isolate spontaneous
426 suppressor mutants, 10^9 BW25113 Δ*tol-pal*$^{\#}$ cells were plated on LB agar plate supplemented with
427 vancomycin (250 μg/ml) and incubated at 37ºC for 48 h. Individual colonies were picked and
428 restreaked on similar plates to verify their vancomycin resistance properties. 36 separate strains
429 were isolated. To identify the genetic location of mutations, whole genome sequencing was
430 performed. Purified genomic DNA was sheared to approximately 300 bp using a focused
431 ultrasonicator (Covaris). A sequencing library was prepared using the TruSeq DNA PCR Free Kit
432 (Illumina) according to the manufacturer's instructions. This was sequenced using a HiSeq 4000
433 with 2×151 bp reads. Raw FASTQ files were mapped to the *E. coli* W3110 genome sequence
434 (NC_007779.1) using bwa (version 0.7.10) (Li & Durbin, 2009); indel realignment and SNP
435 (single nucleotide polymorphism) calling was performed using Lofreq* (version 2.1.2) with
436 default parameters (Wilm et al., 2012). Resulting variants were assigned to associated genes and
437 amino acid changes using the Genbank Refseq W3110 annotation.
438
439 **Antibiotic sensitivity assay.** Sensitivity against different antibiotics was judged by efficiency of
440 plating (EOP) analyses on LB agar plates containing indicated concentrations of drugs.

441 Vancomycin (V1130-1G) and bacitracin (11702-5G) are acquired from Sigma Aldrich. Briefly, 5-
442 ml cultures were grown (inoculated with overnight cultures at 1:100 dilution) in LB broth at 37˚C
443 until OD_{600} reached ~0.6. Cells were normalized according to OD_{600}, first diluted to OD_{600} = 0.1
444 (≈10^8 cells), and then serially diluted in LB with six 10-fold dilutions using 96-well microtiter
445 plates (Corning). Two microliters of the diluted cultures were manually spotted onto the plates and
446 incubated overnight at 37˚C. All results shown are representative of at least three independent
447 replicates.
448
449 **RNase I leakage assay.** Measurement of RNase I leakiness was performed using a plate assay as
450 described before (Lazzaroni & Portalier, 1979). Briefly, 5-ml cultures were grown (inoculated with
451 overnight cultures at 1:100 dilution) in LB broth at 37˚C until OD_{600} reached ~0.6. Cells were
452 normalized to OD_{600} = 0.001, and 2 µl (≈2,000 cells) were manually spotted onto LB agar plates
453 containing 1.9 mg/ml yeast RNA extract (Sigma). The plates were incubated overnight at 37˚C.
454 To precipitate and visualize RNA, the plates were overlaid with cold (12.5% v/v) trichloroacetic
455 acid. Size of the halo were defined as the distance between the edge of the macrocolony and the
456 edge of the halo.
457
458 **Microscopy.** 5-ml cultures were grown (inoculated with overnight cultures at 1:2000 dilution) in
459 LB broth at 37˚C until OD_{600} reached ~0.5 – 0.6. For FM1-43 (Invitrogen) labelling, 1 µg/ml final
460 concentration of the probe was added to 100 µl of bacterial culture before imaging. For
461 vancomycin-BODIPY FL (Invitrogen) labelling, cell cultures were incubated with 10 µg/ml final

462 concentration of the probe for 15 minutes and washed one time with 1 ml fresh LB before
463 resuspended into 200 µl LB. For all experiments, 5 µl of final cell culture were spotted onto freshly
464 prepared 1% LB agarose pads. Images were acquired using a Zeiss LSM710 confocal microscope
465 at 100x magnification. Cells lengths and widths were measured with Image J (Schneider et al.,
466 2012) and result plotted using the *ggplot2* package in R.
467
468 **RT-PCR.** Strains with empty vector or the *uppS/murA* overexpression plasmid were grown in the
469 presence of 25 µM IPTG to mid-log phase. For each strain, total RNA was isolated using RNeasy
470 Mini Kit (Qiagen) and corresponding complementary DNA library was prepared using QuantiTect
471 Reverse Transcription Kit (Qiagen). cDNA sample for each strain was normalized and used as
472 template for PCR amplification using primers specific to *uppS, murA*, and *gyrA* (housekeeping
473 control) for different number of cycles (26, 36, and 23 respectively) to prevent saturation.
474 Following gel electrophoresis, band intensity of the resulting *uppS* and *murA* PCR products was
475 normalized to the corresponding *gyrA* PCR product to obtain the relative gene expression level.
476
477 **σ^E reporter assay.** Strains with plasmid expressing *rpoH*P3::*gfp* or promoterless *gfp* were grown
478 to mid-logarithmic phase ($OD_{600} \approx 0.4$-0.6), then normalized and re-suspended in 150 mM NaCl.
479 Fluorescence level (Ex: 485 nm and Em: 535 nm) of equal amount of cells were measured for each
480 strain using the Victor X4 plate reader (Perkin Elmer). Relative levels of σ^E activation correlates
481 with the expression of GFP due to specific activation of *rpoH*P3 promoter and were determined
482 by normalizing the fluorescence level in strains with *rpoH*P3::*gfp* to the basal fluorescence level

483 in strains expressing *gfp* without promoter. Data from three independent experiments were
484 collected and normalized to the σ^E activation level in WT.
485
486 **Lipid extraction and liquid chromatography-mass spectrometry (LC-MS) analysis.** To
487 prepare the lipid extracts, a modified Bligh and Dyer method was used as described previously
488 (Guan & Maser, 2017). Briefly, bacterial pellets were resuspended in PBS, and
489 chloroform:methanol (1:2, v/v) was added. The mixture was vortexed thoroughly before
490 incubation with shaking at 1,000 rpm, 4°C. Subsequently, water and chloroform were added to
491 each sample to generate a two-phase Bligh-Dyer mixture. The two phases were separated via
492 centrifugation and the lower organic phase was collected in a new tube. The aqueous phase was
493 re-extracted twice with chloroform, and all the organic extracts pooled and dried using a Centrivap
494 and stored at -80°C until use.
495 The lipid samples were reconstituted in chloroform:methanol (1:1, v/v) and analyzed using a
496 high performance chromatography system (1260 Agilent Infinity Quaternary Pump) coupled to an
497 SCIEX QTOF 6600 mass spectrometer in negative electrospray ionization mode. Mass calibration
498 is performed every 5 h, using the automated calibration solution (SCIEX, Canada). For lipid
499 separation, normal phase chromatography was performed as previously described (Guan & Maser,
500 2017). For characterization of the DAG-PP species using tandem mass spectrometry, multiple
501 collision energies ranging from -55 V to -85 V were used. MS and MS/MS spectra obtained were
502 visualized using Peak View (SCIEX) and graphical representations of the selected peaks of
503 interests were plotted using sigmaplot v10.0.

504 **Membrane lipid composition analyses.** Experiments to determine steady-state radiolabeled PL
505 distributions in IMs/OMs and PL/LPS ratios in OMs were adapted from methods previously
506 described with some changes (Shrivastava et al., 2017). Briefly, 10 ml cultures were grown in LB
507 broth (inoculated from overnight culture to a starting OD_{600} of 0.05) containing [^{32}P]-disodium
508 phosphate (final 1 μCi ml^{-1}; Perkin Elmer product no. NEX011001MC) until mid-log phase
509 (OD_{600} ~0.5–0.7). Cells were harvested by centrifugation at 4700 × *g* for 10 min, re-suspended in
510 5 ml of TBS (20 mM pH 8.0 Tris-HCl, 150 mM NaCl), and centrifuged again as above. Resulting
511 cell pellets were re-suspended in 5 ml of 20% sucrose in 10mM Tris-HCl pH 8.0 (w/w) containing
512 1 mM PMSF and 50 μg ml^{-1} DNase I), and lysed by a single passage through a high pressure
513 French press (French Press G-M, Glen Mills) homogenizer at 8000 psi. Unbroken cells were
514 removed by centrifugation at 4700 × *g* for 10 min. The cell lysate was collected, and 5.5 ml of cell
515 lysate was layered on top of a two-step sucrose gradient consisting of 40% sucrose solution (5 ml)
516 layered on top of 65% sucrose solution (1.5 ml) at the bottom of the tube. Samples were centrifuged
517 at 36 000 rpm for 16 h in a Beckman SW41 rotor in an ultracentrifuge (Model XL-90, Beckman).
518 0.8-ml fractions (usually 15 fractions) were manually collected from the top of each tube. IM and
519 OM fractions were pooled and diluted with TBS before centrifugation at 36 000 rpm for one hour
520 in the Beckman SW41 rotor to concentrate the membrane. The resulting membrane pellets (not
521 visible) were resuspended in 320 μl TBS for subsequent extraction of PLs (IM) or PLs and LPS
522 (OM). Protocol for the extraction of PLs and LPS had been described previously (Shrivastava et
523 al., 2017). Dried PLs were resuspended in 50 μl of a mixture of chloroform:methanol (2:1); while
524 dried LPS pellets were resuspended in 50 μl 1% SDS. Equal volumes of PL or LPS solutions were

525 mixed with 2 ml of Ultima Gold scintillation fluid (Perkin Elmer, Singapore) and [^{32}P]-counts
526 were measured using scintillation counting (MicroBeta$^{2®}$, Perkin-Elmer). For each strain,
527 scintillation counts of OM PLs were divided by the total counts of IM PLs and OM PLs to obtain
528 the percentage of OM PLs distribution; while scintillation counts of OM PLs were divided by the
529 counts of OM LPS to obtain the PL/LPS ratio.
530
531 **Quantification of OM vesiculation.** For each strain, 10-ml cells were grown at 37˚C in LB broth
532 (inoculated from an overnight culture at 1:100 dilution) containing [1-^{14}C]-acetate (final 0.2 µCi
533 ml^{-1}; Perkin Elmer product no. NEC084A001MC) until OD600 reached ~0.7. At this OD, cultures
534 were harvested to obtain the cell pellets, and supernatants containing OM vesicles. Cell pellets
535 were washed twice with 10 mM Tris-HCl pH 8.0 and finally suspended in the same buffer (0.2
536 ml). To obtain OM vesicles, supernatants were filtered through 0.45 µm filters followed by
537 ultracentrifugation in a SW41.Ti rotor at 39,000 rpm for 1 h. Finally, the OM vesicles in the
538 resulting pellets were washed and re-suspended in 0.2 ml 10 mM Tris-HCl pH 8.0 buffer.
539 Radioactive counts in cell pellets and OM vesicles were measured after mixing with 2 ml of Ultima
540 Gold scintillation fluid (Perkin Elmer, Singapore). Radioactivity ([^{14}C]-count) was measured on a
541 scintillation counter (MicroBeta$^{2®}$, Perkin-Elmer)
542
543 **SDS-PAGE and immunoblotting.** SDS-PAGE was performed according to Laemmli using the
544 12% or 15% Tris.HCl gels (Laemmli, 1970). For ECA, cell samples were treated with proteinase
545 K (0.25 mg/ml) at 55ºC for 1 h before loading and resolving on 10% Tricine SDS-PAGE gels.

546 Immunoblotting was performed by transferring from the gels onto polyvinylidene fluoride (PVDF)
547 membranes (Immun-Blot® 0.2 µm, Bio-Rad) using the semi-dry electroblotting system (Trans-
548 Blot® TurboTM Transfer System, Bio-Rad). Membranes were blocked using 1X casein blocking
549 buffer (Sigma). Rabbit polyclonal α-ECA_{CYC} antisera (generous gift from Jolanta Lukasiewicz),
550 which reacts with all forms of ECA (ECA_{CYC}, ECA_{LPS}, ECA_{PG}), was used at 1:800 dilution
551 (Gozdzlewicz et al., 2014). α-rabbit IgG secondary antibody conjugated to HRP (from donkey)
552 was purchased from GE Healthcare and used at 1:5,000 dilutions. Luminata Forte Western HRP
553 Substrate (Merck Milipore) was used to develop the membranes and chemiluminescent signals
554 were visualized by G:BOX Chemi XT 4 (Genesys version1.3.4.0, Syngene).

555 **Acknowledgements**

556 We thank Majid Eshaghi (Genome Institute of Singapore, GIS) for providing σ^E reporter
557 plasmids and Kevin Young (University of Arkansas for Medical Sciences) for the generous gifts
558 of the Δ*wcaJ* strain and the *murA* and *uppS* overexpression plasmids. We also thank Kevin Young
559 for critical comments. We are grateful to Jolanta Łukasiewicz (Polish Academy of Sciences) for
560 the α-ECA antibody. WGS work was partially supported by the GIS, and the Singapore Ministry
561 of Health National Medical Research Council (NMRC/CIRG/1357/2013) to S.L.C.. Lipid MS
562 analysis was supported by the Nanyang Assistant Professorship to X.L.G.. All other work were
563 supported by the Singapore Ministry of Education Academic Research Fund Tier 1 Grant, and the
564 Singapore Ministry of Health National Medical Research Council under its Cooperative Basic
565 Research Grant (NMRC/CBRG/0072/2014) to S.-S.C.. The authors declare no conflict of interest.

566

567 **Author contributions**

568 X.E.J., W.B.T., and R.S. performed most of the experiments described in this work; S.L.C.
569 analyzed the whole genome sequencing data of suppressor mutants; D.C.C.S. and X.L.G.
570 performed the MS experiments; S.-S.C. directed and supervised the work; X.E.J., R.S., W.B.T.,
571 and S.-S.C. analyzed the data and wrote the paper; all authors provided critical feedback of the
572 manuscript.

573 **Data availability statement**

574 The data that supports the findings of this study are available in the supplementary material of

575 this article and from the corresponding author upon reasonable request.

576 **References**

577 Acker, G., Bitter-Suermann, D., Meier-Dieter, U., Peters, H., & Mayer, H. (1986).
578 Immunocytochemical localization of enterobacterial common antigen in Escherichia coli
579 and Yersinia enterocolitica cells. *Journal of bacteriology*, *168*(1), 348-356.

580 Baba, T., Ara, T., Hasegawa, M., Takai, Y., Okumura, Y., Baba, M., ... & Mori, H. (2006).
581 Construction of Escherichia coli K-12 in-frame, single-gene knockout mutants: the Keio
582 collection. *Molecular systems biology*, *2*(1), 2006-0008.

583 Barr, K., Klena, J., & Rick, P. D. (1999). The modality of enterobacterial common antigen
584 polysaccharide chain lengths is regulated by o349 of thewec gene cluster of Escherichia
585 coliK-12. *Journal of bacteriology*, *181*(20), 6564-6568.

586 Bernadac, A., Gavioli, M., Lazzaroni, J. C., Raina, S., & Lloubès, R. (1998). Escherichia coli tol-
587 pal mutants form outer membrane vesicles. *Journal of bacteriology*, *180*(18), 4872-4878.

588 Campos, M., Govers, S. K., Irnov, I., Dobihal, G. S., Cornet, F., & Jacobs-Wagner, C. (2018).
589 Genomewide phenotypic analysis of growth, cell morphogenesis, and cell cycle events in
590 Escherichia coli. *Molecular systems biology*, *14*(6), e7573.

591 Casadaban, M. J. (1976). Transposition and fusion of the lac genes to selected promoters in
592 Escherichia coli using bacteriophage lambda and Mu. *Journal of molecular biology*, *104*(3),
593 541-555.

594 Cascales, E., Gavioli, M., Sturgis, J. N., & Lloubès, R. (2000). Proton motive force drives the
595 interaction of the inner membrane TolA and outer membrane pal proteins in Escherichia
596 coli. *Molecular microbiology*, *38*(4), 904-915.

597 Castelli, M. E., & Véscovi, E. G. (2011). The Rcs signal transduction pathway is triggered by
598 enterobacterial common antigen structure alterations in Serratia marcescens. *Journal of*
599 *bacteriology*, *193*(1), 63-74.
600 Cherepanov, P. P., & Wackernagel, W. (1995). Gene disruption in Escherichia coli: TcR and KmR
601 cassettes with the option of Flp-catalyzed excision of the antibiotic-resistance
602 determinant. *Gene*, *158*(1), 9-14.
603 Clavel, T., Lazzaroni, J. C., Vianney, A., & Portalier, R. (1996). Expression of the tolQRA genes
604 of Escherichia coli K-12 is controlled by the RcsC sensor protein involved in capsule
605 synthesis. *Molecular microbiology*, *19*(1), 19-25.
606 Danese, P. N., Oliver, G. R., Barr, K., Bowman, G. D., Rick, P. D., & Silhavy, T. J. (1998).
607 Accumulation of the Enterobacterial Common Antigen Lipid II Biosynthetic Intermediate
608 StimulatesdegP Transcription in Escherichia coli. *Journal of bacteriology*, *180*(22), 5875-
609 5884.
610 Datsenko, K. A., & Wanner, B. L. (2000). One-step inactivation of chromosomal genes in
611 Escherichia coli K-12 using PCR products. *Proceedings of the National Academy of*
612 *Sciences*, *97*(12), 6640-6645.
613 Donohue-Rolfe, A. M., & Schaechter, M. (1980). Translocation of phospholipids from the inner
614 to the outer membrane of Escherichia coli. *Proceedings of the National Academy of*
615 *Sciences*, *77*(4), 1867-1871.

616 Ekiert, D. C., Bhabha, G., Isom, G. L., Greenan, G., Ovchinnikov, S., Henderson, I. R., ... & Vale,
617 R. D. (2017). Architectures of lipid transport systems for the bacterial outer
618 membrane. *Cell*, *169*(2), 273-285.
619 Ercan, B., Low, W. Y., Liu, X., & Chng, S. S. (2018). Characterization of interactions and
620 phospholipid transfer between substrate binding proteins of the OmpC-mla
621 system. *Biochemistry*, *58*(2), 114-119.
622 Feldman, M. F., Marolda, C. L., Monteiro, M. A., Perry, M. B., Parodi, A. J., & Valvano, M. A.
623 (1999). The activity of a putative polyisoprenol-linked sugar translocase (Wzx) involved in
624 Escherichia coli O antigen assembly is independent of the chemical structure of the O
625 repeat. *Journal of Biological Chemistry*, *274*(49), 35129-35138.
626 Gerding, M. A., Ogata, Y., Pecora, N. D., Niki, H., & De Boer, P. A. (2007). The trans-envelope
627 Tol–Pal complex is part of the cell division machinery and required for proper outer-
628 membrane invagination during cell constriction in E. coli. *Molecular microbiology*, *63*(4),
629 1008-1025.
630 Gozdziewicz, T. K., Lugowski, C., & Lukasiewicz, J. (2014). First evidence for a covalent linkage
631 between enterobacterial common antigen and lipopolysaccharide in Shigella sonnei phase II
632 ECALPS. *Journal of Biological Chemistry*, *289*(5), 2745-2754.
633 Guan, X. L., & Mäser, P. (2017). Comparative sphingolipidomics of disease-causing
634 trypanosomatids reveal unique lifecycle-and taxonomy-specific lipid chemistries. *Scientific*
635 *reports*, *7*(1), 1-13.

636 Hagan, C. L., Silhavy, T. J., & Kahne, D. (2011). β-Barrel membrane protein assembly by the Bam
637 complex. *Annual review of biochemistry*, *80*, 189-210.
638 Hughes, G. W., Hall, S. C., Laxton, C. S., Sridhar, P., Mahadi, A. H., Hatton, C., ... & Jamshad,
639 M. (2019). Evidence for phospholipid export from the bacterial inner membrane by the Mla
640 ABC transport system. *Nature Microbiology*, *4*(10), 1692-1705.
641 Jones, N. C., & Osborn, M. J. (1977). Translocation of phospholipids between the outer and inner
642 membranes of Salmonella typhimurium. *Journal of Biological Chemistry*, *252*(20), 7405-
643 7412.
644 Jorgenson, M. A., Kannan, S., Laubacher, M. E., & Young, K. D. (2016). Dead-end intermediates
645 in the enterobacterial common antigen pathway induce morphological defects in Escherichia
646 coli by competing for undecaprenyl phosphate. *Molecular microbiology*, *100*(1), 1-14.
647 Jorgenson, M. A., & Young, K. D. (2016). Interrupting biosynthesis of O antigen or the
648 lipopolysaccharide core produces morphological defects in Escherichia coli by sequestering
649 undecaprenyl phosphate. *Journal of bacteriology*, *198*(22), 3070-3079.
650 Kajimura, J., Rahman, A., & Rick, P. D. (2005). Assembly of cyclic enterobacterial common
651 antigen in Escherichia coli K-12. *Journal of bacteriology*, *187*(20), 6917-6927.
652 Kamemoto, Y., Funaba, N., Kawakami, M., Sawasato, K., Kanno, K., Suzuki, S., ... & Nishiyama,
653 K. I. (2019). Biosynthesis of glycolipid MPIase (membrane protein integrase) is independent
654 of the genes for ECA (enterobacterial common antigen). *The Journal of general and applied*
655 *microbiology*.

656 Khetrapal, V., Mehershahi, K., Rafee, S., Chen, S., Lim, C. L., & Chen, S. L. (2015). A set of
657 powerful negative selection systems for unmodified Enterobacteriaceae. *Nucleic acids*
658 *research*, *43*(13), e83-e83.
659 Krishnamoorthy, G., Wolloscheck, D., Weeks, J. W., Croft, C., Rybenkov, V. V., & Zgurskaya,
660 H. I. (2016). Breaking the permeability barrier of Escherichia coli by controlled
661 hyperporination of the outer membrane. *Antimicrobial agents and chemotherapy*, *60*(12),
662 7372-7381.
663 Kuhn, H. M., Meier-Dieter, U., & Mayer, H. (1988). ECA, the enterobacterial common
664 antigen. *FEMS microbiology reviews*, *4*(3), 195-222.
665 Kuhn, H. M., Neter, E., & Mayer, H. (1983). Modification of the lipid moiety of the enterobacterial
666 common antigen by the" Pseudomonas factor". *Infection and immunity*, *40*(2), 696-700.
667 Laemmli, U. K. (1970). Cleavage of structural proteins during the assembly of the head of
668 bacteriophage T4. *nature*, *227*(5259), 680-685.
669 Langley, K. E., Hawrot, E., & Kennedy, E. P. (1982). Membrane assembly: movement of
670 phosphatidylserine between the cytoplasmic and outer membranes of Escherichia
671 coli. *Journal of bacteriology*, *152*(3), 1033-1041.
672 Lazzaroni, J. C., Portalier, R. C., & Atlan, D. (1979). Isolation and preliminary characterization of
673 periplasmic-leaky mutants of Escherichia coli K-12. *FEMS Microbiology Letters*, *5*(6), 411-
674 416.
675 Li, H., & Durbin, R. (2009). Fast and accurate short read alignment with Burrows–Wheeler
676 transform. *bioinformatics*, *25*(14), 1754-1760.

677 Lloubès, R., Cascales, E., Walburger, A., Bouveret, E., Lazdunski, C., Bernadac, A., & Journet,
678 L. (2001). The Tol-Pal proteins of the Escherichia coli cell envelope: an energized system
679 required for outer membrane integrity?. *Research in microbiology*, *152*(6), 523-529.
680 Masilamani, R., Cian, M. B., & Dalebroux, Z. D. (2018). Salmonella Tol-Pal reduces outer
681 membrane glycerophospholipid levels for envelope homeostasis and survival during
682 bacteremia. *Infection and immunity*, *86*(7).
683 McMahon, K. J., Castelli, M. E., Vescovi, E. G., & Feldman, M. F. (2012). Biogenesis of outer
684 membrane vesicles in Serratia marcescens is thermoregulated and can be induced by
685 activation of the Rcs phosphorelay system. *Journal of bacteriology*, *194*(12), 3241-3249.
686 Meier-Dieter, U., Starman, R., Barr, K., Mayer, H., & Rick, P. D. (1990). Biosynthesis of
687 enterobacterial common antigen in Escherichia coli. Biochemical characterization of Tn10
688 insertion mutants defective in enterobacterial common antigen synthesis. *Journal of*
689 *Biological Chemistry*, *265*(23), 13490-13497.
690 Mitchell, A. M., Srikumar, T., & Silhavy, T. J. (2018). Cyclic enterobacterial common antigen
691 maintains the outer membrane permeability barrier of Escherichia coli in a manner controlled
692 by YhdP. *MBio*, *9*(4).
693 Nikaido, H. (2003). Molecular basis of bacterial outer membrane permeability
694 revisited. *Microbiology and molecular biology reviews*, *67*(4), 593-656.
695 Nikaido, H. (2005). Restoring permeability barrier function to outer membrane. *Chemistry &*
696 *biology*, *12*(5), 507-509.

697 Nishiyama, K. I., Maeda, M., Yanagisawa, K., Nagase, R., Komura, H., Iwashita, T., ... &
698 Shimamoto, K. (2012). MPIase is a glycolipozyme essential for membrane protein
699 integration. *Nature communications*, *3*(1), 1-10.
700 Okuda, S., Sherman, D. J., Silhavy, T. J., Ruiz, N., & Kahne, D. (2016). Lipopolysaccharide
701 transport and assembly at the outer membrane: the PEZ model. *Nature Reviews*
702 *Microbiology*, *14*(6), 337-345.
703 Okuda, S., & Tokuda, H. (2011). Lipoprotein sorting in bacteria. *Annual review of*
704 *microbiology*, *65*, 239-259.
705 Oursel, D., Loutelier-Bourhis, C., Orange, N., Chevalier, S., Norris, V., & Lange, C. M. (2007).
706 Lipid composition of membranes of Escherichia coli by liquid chromatography/tandem mass
707 spectrometry using negative electrospray ionization. *Rapid Communications in Mass*
708 *Spectrometry: An International Journal Devoted to the Rapid Dissemination of Up-to-the-*
709 *Minute Research in Mass Spectrometry*, *21*(11), 1721-1728.
710 Raetz, C. R., & Whitfield, C. (2002). Lipopolysaccharide endotoxins. *Annual review of*
711 *biochemistry*, *71*(1), 635-700.
712 Rahman, A., Barr, K., & Rick, P. D. (2001). Identification of the Structural Gene for the TDP-
713 Fuc4NAc: Lipid II Fuc4NAc Transferase Involved in Synthesis of Enterobacterial Common
714 Antigen in Escherichia coliK-12. *Journal of bacteriology*, *183*(22), 6509-6516.
715 Raivio, T. L., Popkin, D. L., & Silhavy, T. J. (1999). The Cpx envelope stress response is controlled
716 by amplification and feedback inhibition. *Journal of bacteriology*, *181*(17), 5263-5272.

717 Ramos-Morales, F., Prieto, A. I., Beuzón, C. R., Holden, D. W., & Casadesús, J. (2003). Role for
718 Salmonella enterica enterobacterial common antigen in bile resistance and
719 virulence. *Journal of bacteriology*, *185*(17), 5328-5332.
720 Rassam, P., Long, K. R., Kaminska, R., Williams, D. J., Papadakos, G., Baumann, C. G., &
721 Kleanthous, C. (2018). Intermembrane crosstalk drives inner-membrane protein
722 organization in Escherichia coli. *Nature communications*, *9*(1), 1-8.
723 Rick, P. D., Barr, K., Sankaran, K., Kajimura, J., Rush, J. S., & Waechter, C. J. (2003). Evidence
724 that the wzxE gene of Escherichia coli K-12 encodes a protein involved in the transbilayer
725 movement of a trisaccharide-lipid intermediate in the assembly of enterobacterial common
726 antigen. *Journal of Biological Chemistry*, *278*(19), 16534-16542.
727 Rick, P. D., Hubbard, G. L., Kitaoka, M., Nagaki, H., Kinoshita, T., Dowd, S., ... & Ho, C. (1998).
728 Characterization of the lipid-carrier involved in the synthesis of enterobacterial common
729 antigen (ECA) and identification of a novel phosphoglyceride in a mutant of Salmonella
730 typhimurium defective in ECA synthesis. *Glycobiology*, *8*(6), 557-567.
731 Rinno, J., Golecki, J. R., & Mayer, H. (1980). Localization of enterobacterial common antigen:
732 immunogenic and nonimmunogenic enterobacterial common antigen-containing
733 Escherichia coli. *Journal of bacteriology*, *141*(2), 814-821.
734 Rojas, E. R., Billings, G., Odermatt, P. D., Auer, G. K., Zhu, L., Miguel, A., ... & Huang, K. C.
735 (2018). The outer membrane is an essential load-bearing element in Gram-negative
736 bacteria. *Nature*, *559*(7715), 617-621.

737 Ruan, X., Monjarás Feria, J., Hamad, M., & Valvano, M. A. (2018). Escherichia coli and
738 Pseudomonas aeruginosa lipopolysaccharide O-antigen ligases share similar membrane
739 topology and biochemical properties. *Molecular microbiology*, *110*(1), 95-113.
740 Ruiz, N., Gronenberg, L. S., Kahne, D., & Silhavy, T. J. (2008). Identification of two inner-
741 membrane proteins required for the transport of lipopolysaccharide to the outer membrane
742 of Escherichia coli. *Proceedings of the National Academy of Sciences*, *105*(14), 5537-5542.
743 Ruiz, N., Wu, T., Kahne, D., & Silhavy, T. J. (2006). Probing the barrier function of the outer
744 membrane with chemical conditionality. *ACS chemical biology*, *1*(6), 385-395.
745 Sawasato, K., Sato, R., Nishikawa, H., Iimura, N., Kamemoto, Y., Fujikawa, K., ... & Ueda, T.
746 (2019a). CdsA is involved in biosynthesis of glycolipid MPIase essential for membrane
747 protein integration in vivo. *Scientific reports*, *9*.
748 Sawasato, K., Suzuki, S., & Nishiyama, K. I. (2019b). Increased expression of the bacterial
749 glycolipid MPIase is required for efficient protein translocation across membranes in cold
750 conditions. *Journal of Biological Chemistry*, *294*(21), 8403-8411.
751 Schmidt, G., Mannel, D., Mayer, H., Whang, H. Y., & Neter, E. (1976). Role of a
752 lipopolysaccharide gene for immunogenicity of the enterobacterial common
753 antigen. *Journal of Bacteriology*, *126*(2), 579-586.
754 Schneider, C. A., Rasband, W. S., & Eliceiri, K. W. (2012). NIH Image to ImageJ: 25 years of
755 image analysis. *Nature methods*, *9*(7), 671-675.
756 Shrivastava, R., & Chng, S. S. (2019). Lipid trafficking across the Gram-negative cell
757 envelope. *Journal of Biological Chemistry*, *294*(39), 14175-14184.

758 Shrivastava, R., Jiang, X. E., & Chng, S. S. (2017). Outer membrane lipid homeostasis via
759 retrograde phospholipid transport in Escherichia coli. *Molecular microbiology*, *106*(3), 395-
760 408.
761 Silhavy, T. J., Berman, M. L., & Enquist, L. W. (1984). *Experiments with gene fusions*. Cold
762 Spring Harbor Laboratory.
763 Stevenson, G., Andrianopoulos, K., Hobbs, M., & Reeves, P. R. (1996). Organization of the
764 Escherichia coli K-12 gene cluster responsible for production of the extracellular
765 polysaccharide colanic acid. *Journal of bacteriology*, *178*(16), 4885-4893.
766 Stokes, J. M., French, S., Ovchinnikova, O. G., Bouwman, C., Whitfield, C., & Brown, E. D.
767 (2016). Cold stress makes Escherichia coli susceptible to glycopeptide antibiotics by altering
768 outer membrane integrity. *Cell chemical biology*, *23*(2), 267-277.
769 Stout, V., & Gottesman, S. (1990). RcsB and RcsC: a two-component regulator of capsule
770 synthesis in Escherichia coli. *Journal of bacteriology*, *172*(2), 659-669.
771 Sturgis, J. N. (2001). Organisation and evolution of the tol-pal gene cluster. *Journal of molecular*
772 *microbiology and biotechnology*, *3*(1), 113-122.
773 Thong, S., Ercan, B., Torta, F., Fong, Z. Y., Wong, H. Y. A., Wenk, M. R., & Chng, S. S. (2016).
774 Defining key roles for auxiliary proteins in an ABC transporter that maintains bacterial outer
775 membrane lipid asymmetry. *Elife*, *5*, e19042.
776 Trisler, P., & Gottesman, S. (1984). lon transcriptional regulation of genes necessary for capsular
777 polysaccharide synthesis in Escherichia coli K-12. *Journal of Bacteriology*, *160*(1), 184-
778 191.

779 Wilm, A., Aw, P. P. K., Bertrand, D., Yeo, G. H. T., Ong, S. H., Wong, C. H., ... & Nagarajan, N.
780 (2012). LoFreq: a sequence-quality aware, ultra-sensitive variant caller for uncovering cell-
781 population heterogeneity from high-throughput sequencing datasets. *Nucleic acids*
782 *research*, *40*(22), 11189-11201.
783 Yakhnina, A. A., & Bernhardt, T. G. (2020). The Tol-Pal system is required for peptidoglycan-
784 cleaving enzymes to complete bacterial cell division. *Proceedings of the National Academy*
785 *of Sciences*, *117*(12), 6777-6783.

786 **Figures**

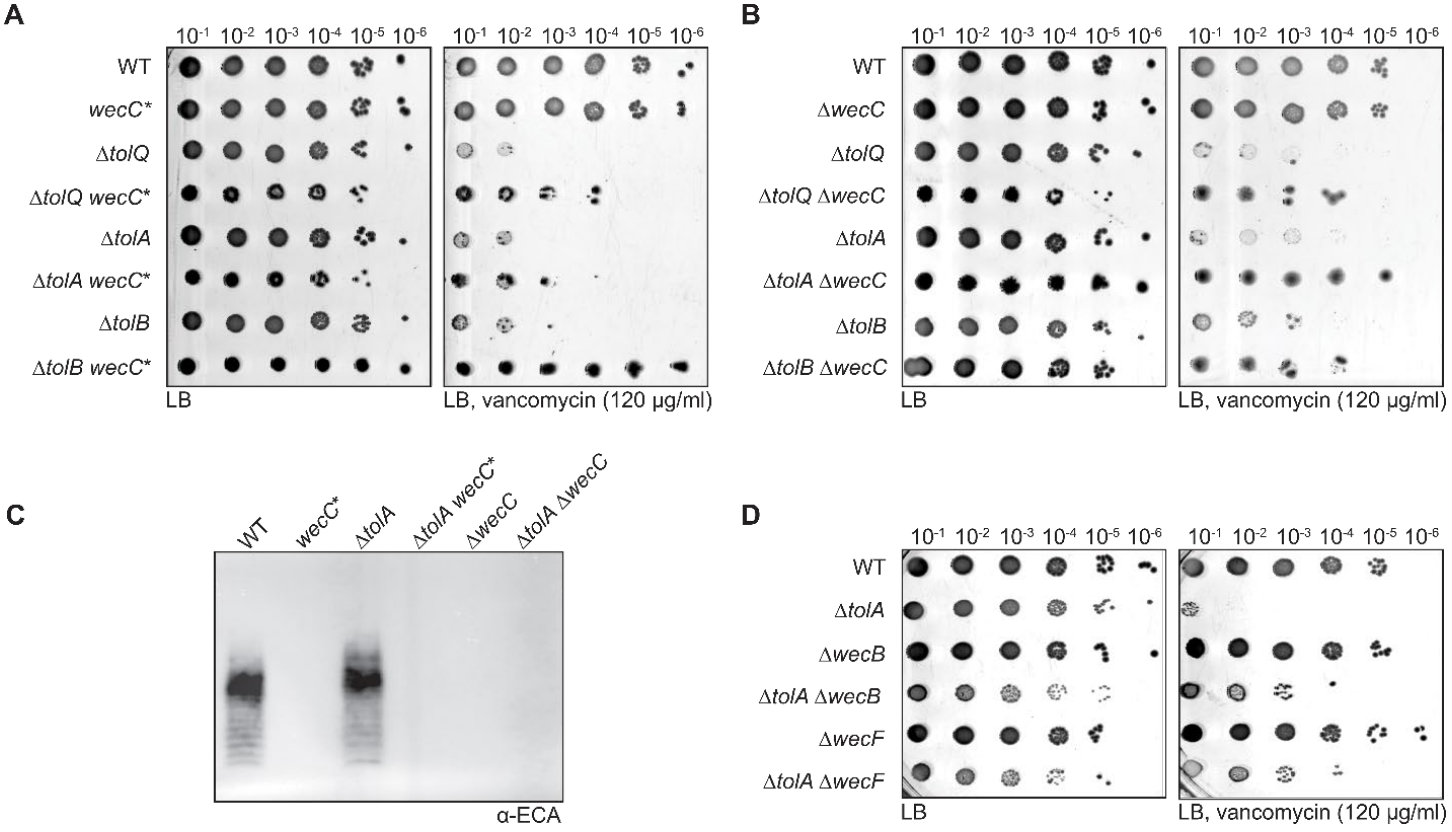

787

788 **Fig. 1** Loss-of-function mutations in the ECA pathway rescue vancomycin sensitivity in *tol-pal*
789 mutants. Vancomycin sensitivity of indicated *tol-pal* strains with or without (A) *wecC**, (B)
790 Δ*wecC*, and (D) Δ*wecB*/Δ*wecF* mutations based on efficiency of plating (EOP) on LB agar plates
791 supplemented with vancomycin (120 µg/ml). (C) ECA levels in wild-type (WT) and Δ*tolA* strains
792 with or without *wecC** and Δ*wecC* mutations as judged by immunoblot analysis using α-ECA
793 antibody. Samples were normalized by OD_{600} and treated with proteinase K prior to Tricine SDS-
794 PAGE/immunoblotting.

795

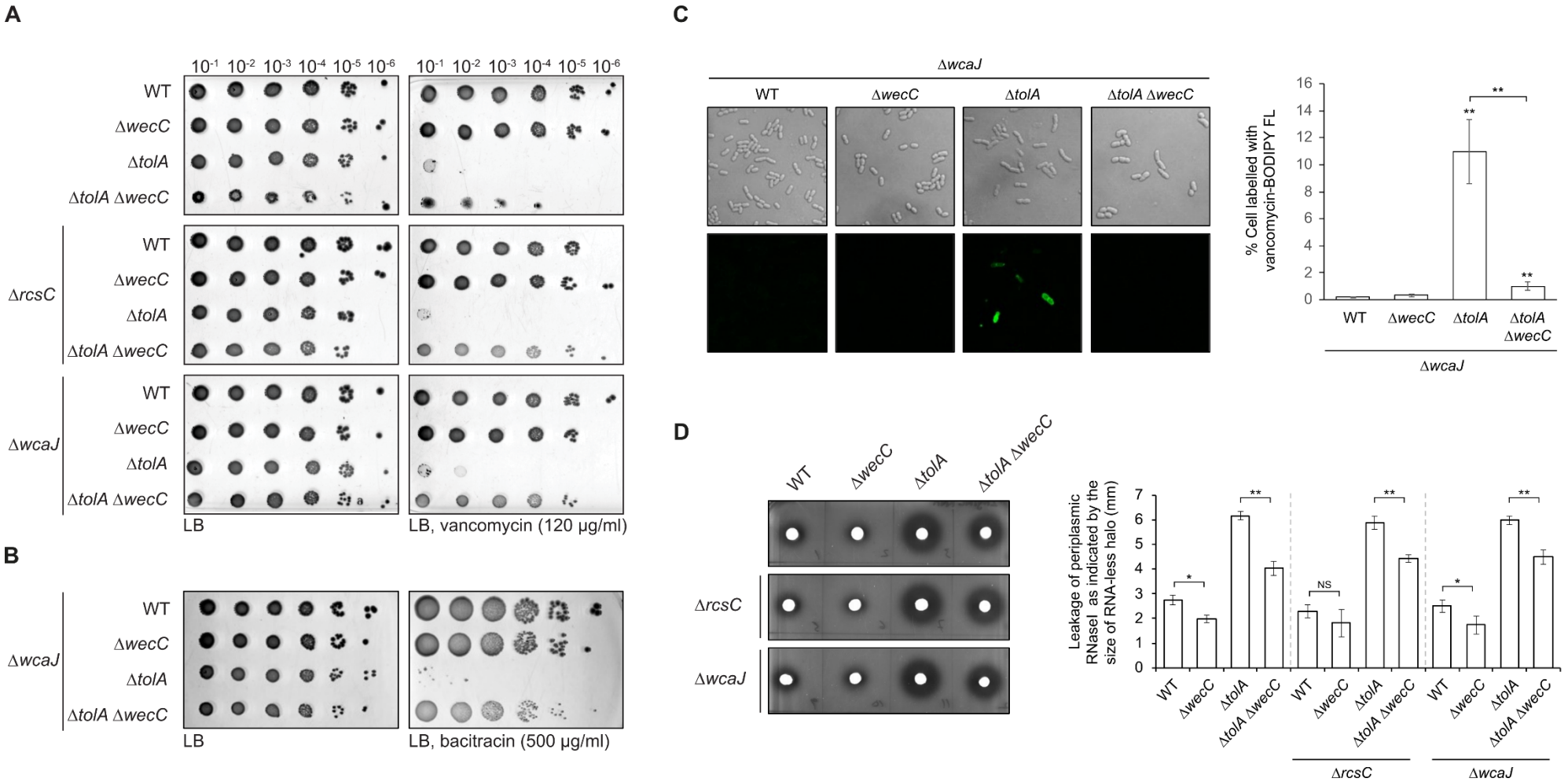
A
10-1 10-2 10-3 10-4 10-5 10-6
WT
ΔwecC
ΔtolA
ΔtolA ΔwecC
ΔrcsC
ΔwcaJ
LB
LB, vancomycin (120 µg/ml)
B
LB, bacitracin (500 µg/ml)
C
ΔwcaJ
% Cell labelled with vancomycin-BODIPY FL
D
Leakage of periplasmic RNaseI as indicated by the size of RNA-less halo (mm)
NS

796 **Fig. 2** Restoration of OM permeability defects by Δ*wecC* in cells lacking TolA does not require
797 the Rcs phosphorelay cascade and/or capsular polysaccharide biosynthesis. (A) Vancomycin
798 sensitivity of indicated strains in either Δ*rcsC* or Δ*wcaJ* backgrounds based on EOP on LB agar
799 plates supplemented with vancomycin (120 μg/ml). (B) Bacitracin sensitivity of indicated strains
800 in Δ*wcaJ* backgrounds based on EOP on LB agar plates supplemented with bacitracin (500 μg/ml,
801 ⩾60 U/mg). (C) Confocal microscopy images of indicated strains (Δ*wcaJ* background) after
802 incubation with BODIPY FL vancomycin. Quantification of the percentage of cells
803 circumferentially labelled with BODIPY FL vancomycin from different fields of view (n = 6) is
804 shown on the right; error bars represent standard deviation. Student's t-tests: $**$, $p < 0.005$ (as
805 compared to WT, unless otherwise indicated). (D) RNase I leakage in the same strains as (A), as
806 judged by RNA degradation (halo formation) around cells spotted on LB agar plates containing
807 yeast RNA, subsequently precipitated with trichloroacetic acid. Quantification of the distances
808 between the edges of the macrocolony and the halo (n = 3) is shown on the right; error bars
809 represent standard deviation. Student's t-tests: *, $p < 0.05$; **, $p < 0.005$.

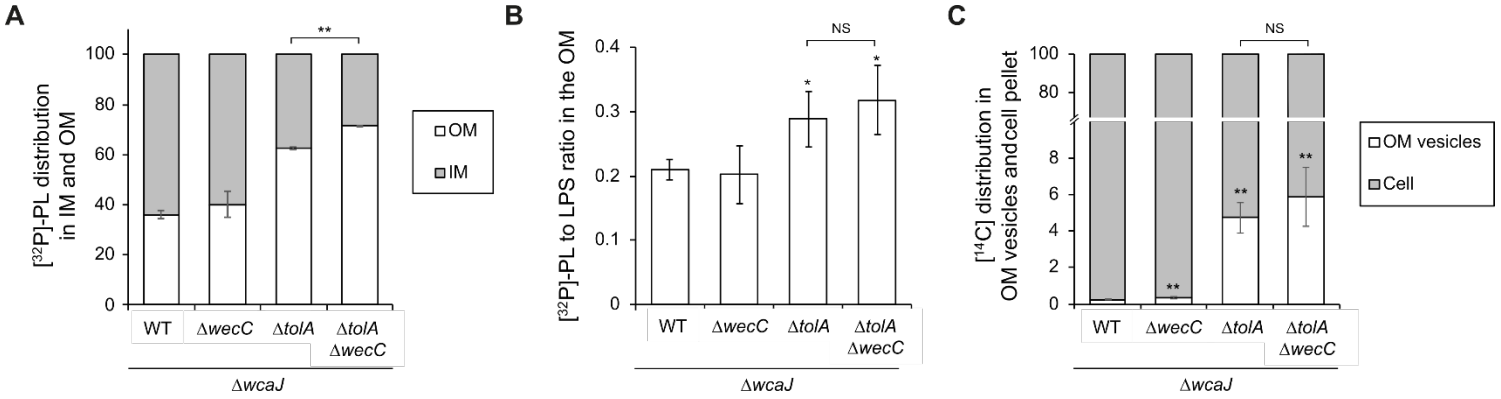

Fig. 3 Δ*wecC* mutation does not restore OM lipid homeostasis in cells lacking TolA. (A) Steady-state [^{32}P]-labelled PL distribution profiles of indicated Δ*wcaJ* strains. Cells were grown in the presence of [^{32}P]-phosphate to label PLs in the IMs and OMs. [^{32}P]-scintillation counts detected in PLs extracted from IM and OM fractions were expressed as a percentage of their sums, averaged across three replicate experiments. (B) Steady-state PL:LPS ([^{32}P]-phosphate labelled) ratios in the OMs of indicated Δ*wcaJ* strains. Arbitrary OM PL:LPS ratios were calculated based on [^{32}P]-scintillation counts detected from PL or LPS, differentially extracted from the OM fractions of the indicated strains. (C) Steady-state distribution of [^{14}C]-acetate-labelled lipids found associated with cells (total membranes) or OM vesicles for the indicated strains. Error bars represent standard deviations calculated from triplicate experiments. Student's t-tests: *, $p < 0.05$; **, $p < 0.005$; NS, not significant (as compared to WT, unless otherwise indicated).

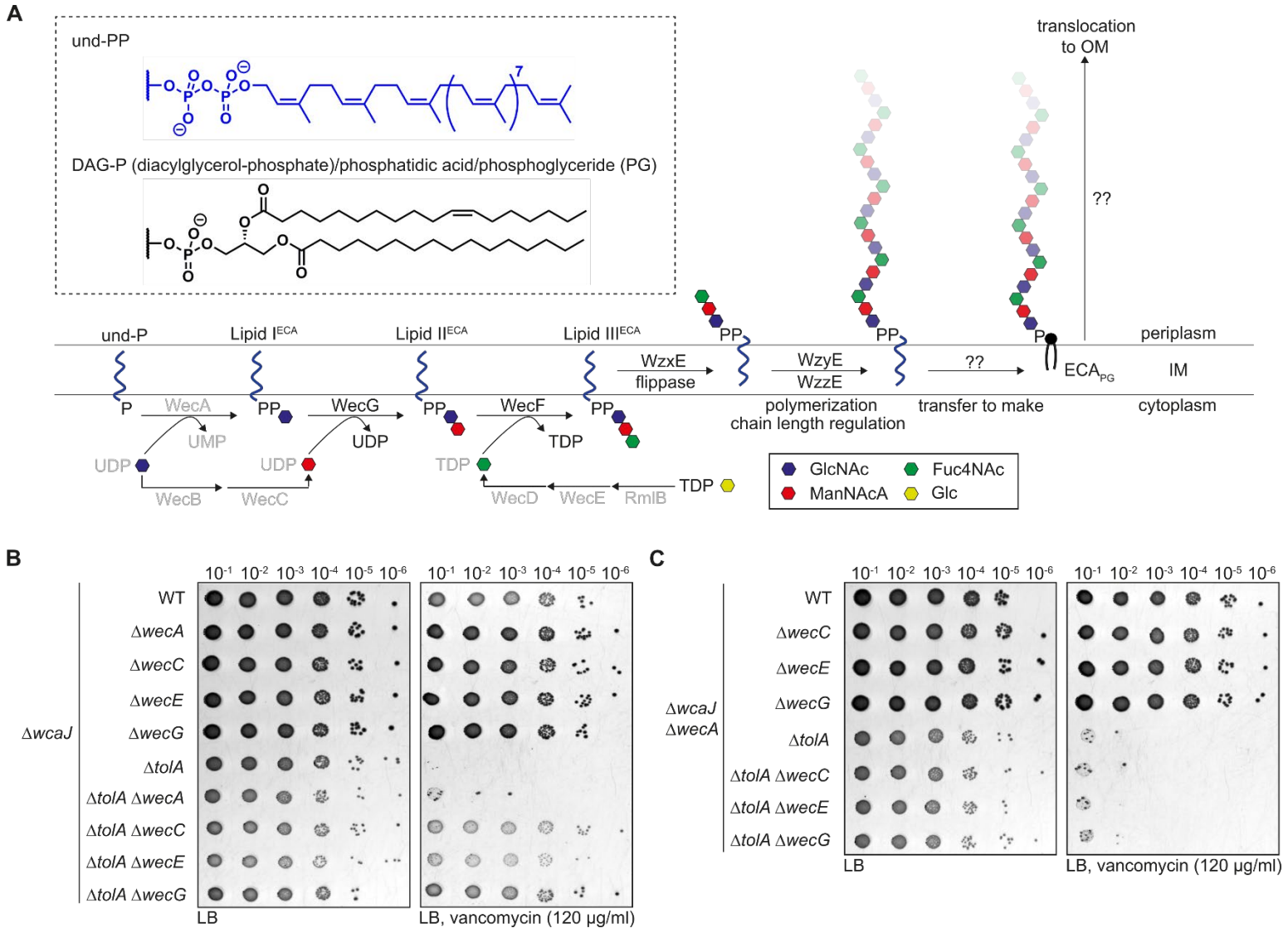

Fig. 4 Accumulation of ECA biosynthetic intermediates restores vancomycin resistance in cells lacking TolA. (A) Schematic of the ECA biosynthetic pathway illustrating und-PP-GlcNAc-ManNAcA-Fuc4NAc (Lipid III^{ECA}) synthesis at the inner leaflet of IM, and subsequent polymerization at the outer leaflet. The final ECA polymer (ECA_{PG}) is attached to a phosphoglyceride (i.e. diacylglycerol-phosphate (DAG-P) aka phosphatidic acid) and transported to the OM. Chemical structures of und-PP and DAG-P anchors are shown. (B, C) Vancomycin sensitivity of the Δ*wcaJ* Δ*tolA* strain with or without indicated *wec* mutations in otherwise (B) WT

828 or (C) Δ*wecA* backgrounds, based on efficiency of plating (EOP) on LB agar plates supplemented

829 with vancomycin (120 ug/ml).

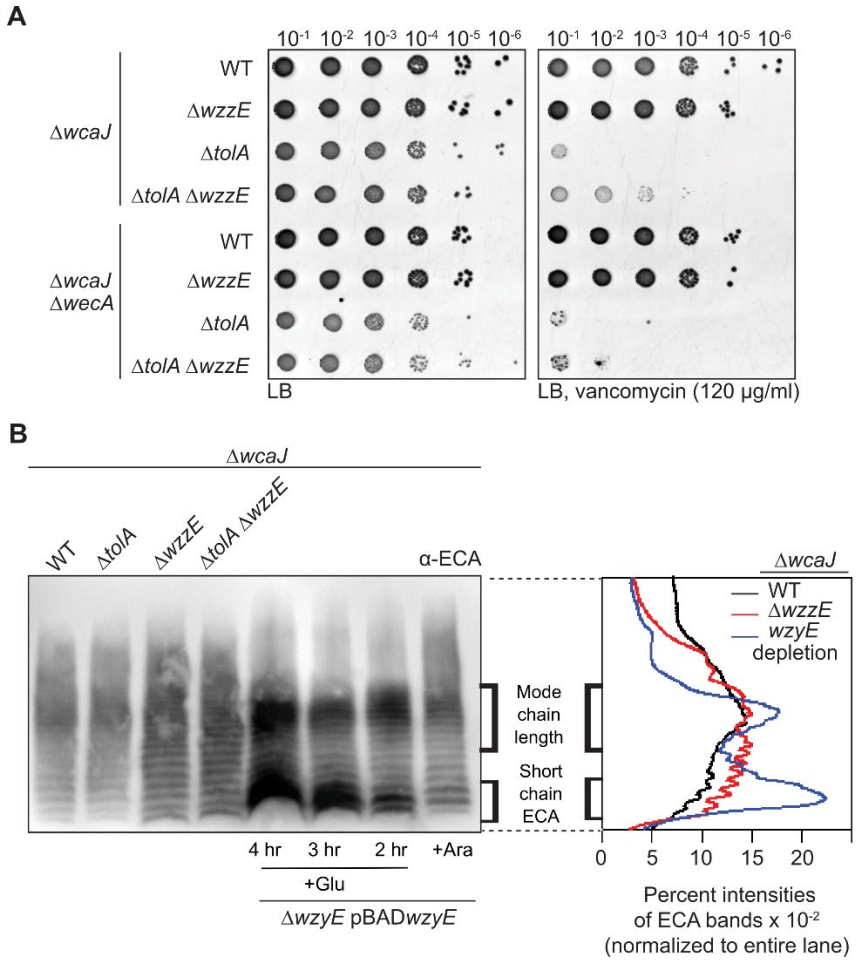

Fig. 5 Partial accumulation of Lipid III^{ECA} and/or short chain ECA rescues vancomycin sensitivity in cells lacking TolA. (A) Vancomycin sensitivity of the Δ*wcaJ* Δ*tolA* strain with or without Δ*wzzE* mutation in otherwise WT or Δ*wecA* backgrounds, based on efficiency of plating (EOP) on LB agar plates supplemented with vancomycin (120 ug/ml). (B) ECA profiles in the indicated Δ*wcaJ* strains as judged by immunoblot analysis using α-ECA antibody. Samples were normalized by OD_{600} and treated with proteinase K prior to Tricine SDS-PAGE/immunoblotting. Profiles in strains progressively depleted of *wzyE* (at 2, 3, or 4 hours post subculture into media containing 0.2% glucose) are used to visualize accumulation of Lipid III^{ECA}. Relative band intensities from ECA profiles of WT, Δ*wzzE,* and *wzyE*-depleted (for 3 hr) strains are shown on the right.

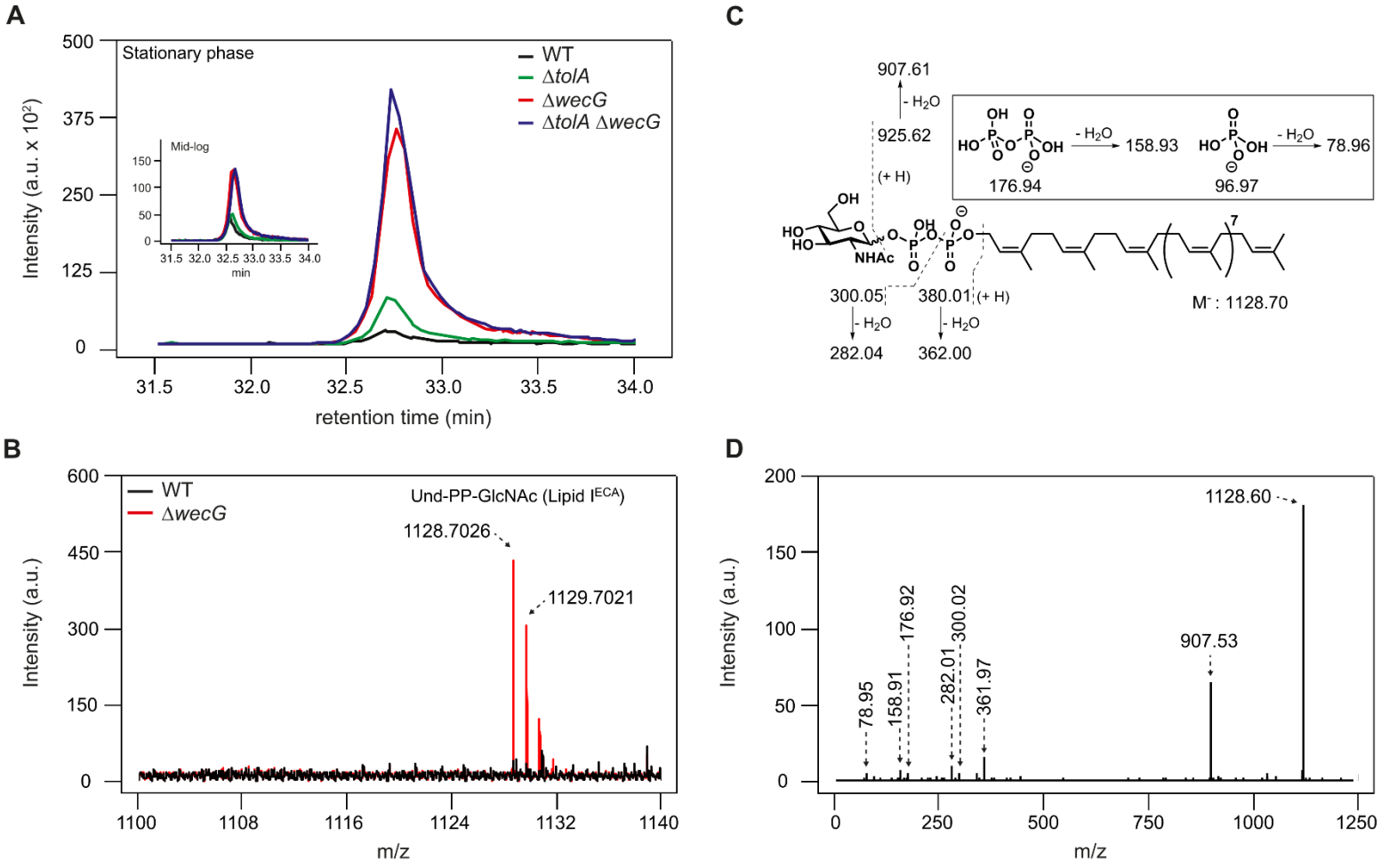

Fig. 6 Strains lacking WecG accumulate und-PP-GlcNAc (Lipid I^{ECA}) intermediates. (A) Ion chromatograms (XICs) of und-PP-GlcNAc (m/z 1128.7026) extracted from LC-MS analyses of total lipids isolated from indicated Δ*wcaJ* strains grown to stationary phase. Inset, corresponding XICs for the same lipid in strains grown to mid-logorithmic phase. (B) Mass spectra obtained from integration of XIC peak region in (A) of Δ*wcaJ* (WT) and Δ*wcaJ* Δ*wecG* strains. WT peaks (black) are overlaid on top of Δ*wecG* peaks (red), illustrating strong und-PP-GlcNAc signals in the latter strain. (C) Proposed fragmentation pattern with mass assignments, and (D) MS/MS spectrum at low collision energy (-55V) of the und-PP-GlcNAc species.

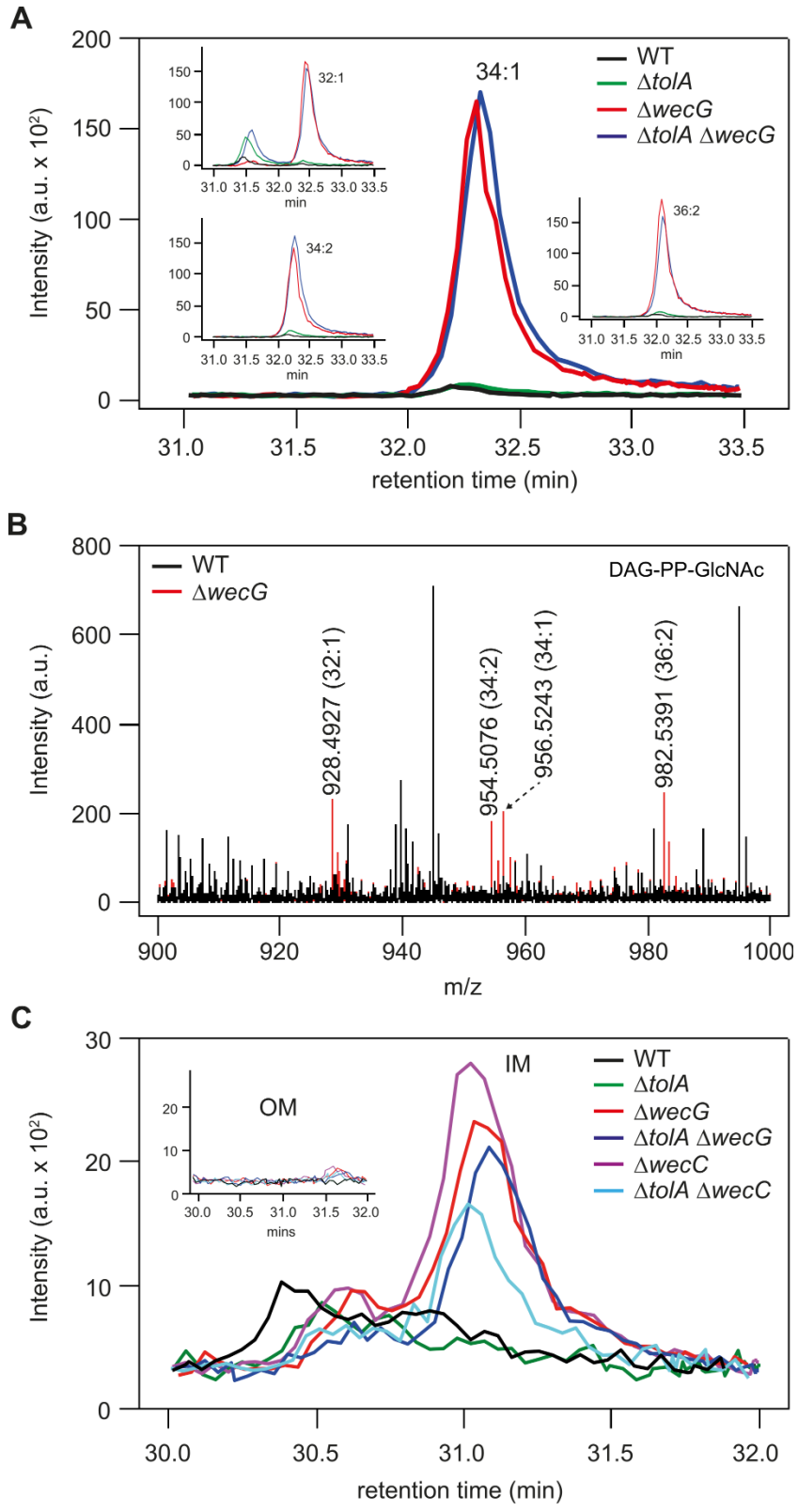
A
Intensity (a.u. x 10²)
retention time (min)
34:1
32:1
34:2
36:2
min
WT
ΔtolA
ΔwecG
ΔtolA ΔwecG
B
Intensity (a.u.)
m/z
WT
ΔwecG
DAG-PP-GlcNAc
928.4927 (32:1)
954.5076 (34:2)
956.5243 (34:1)
982.5391 (36:2)
C
Intensity (a.u. x 10²)
retention time (min)
IM
OM
mins
WT
ΔtolA
ΔwecG
ΔtolA ΔwecG
ΔwecC
ΔtolA ΔwecC

848

849 **Fig. 7** Strains lacking WecG or WecC accumulate DAG-PP-GlcNAc species in the IM. (A) Ion
850 chromatograms (XICs) of 34:1 DAG-PP-GlcNAc (m/z 956.5243) extracted from LC-MS analyses
851 of total lipids isolated from indicated Δ*wcaJ* strains grown to mid-logarithmic phase. Inset, XICs
852 of corresponding 32:1 (m/z 928.4927), 34:2 (954.5076) and 36:1 (m/z 982.5391) species. Data
853 from stationary phase samples are similar. (B) Mass spectra obtained from integration of XIC peak
854 region in (A) of Δ*wcaJ* (WT) and Δ*wcaJ* Δ*wecG* strains. WT peaks (black) are overlaid on top of
855 Δ*wecG* peaks (red), illustrating unique DAG-PP-GlcNAc signals in the latter strain. (C) XICs of
856 34:1 DAG-PP-GlcNAc (m/z 956.5243) extracted from LC-MS analyses of IM lipids isolated from
857 indicated Δ*wcaJ* strains. Inset, XICs of the same species from OM lipids.

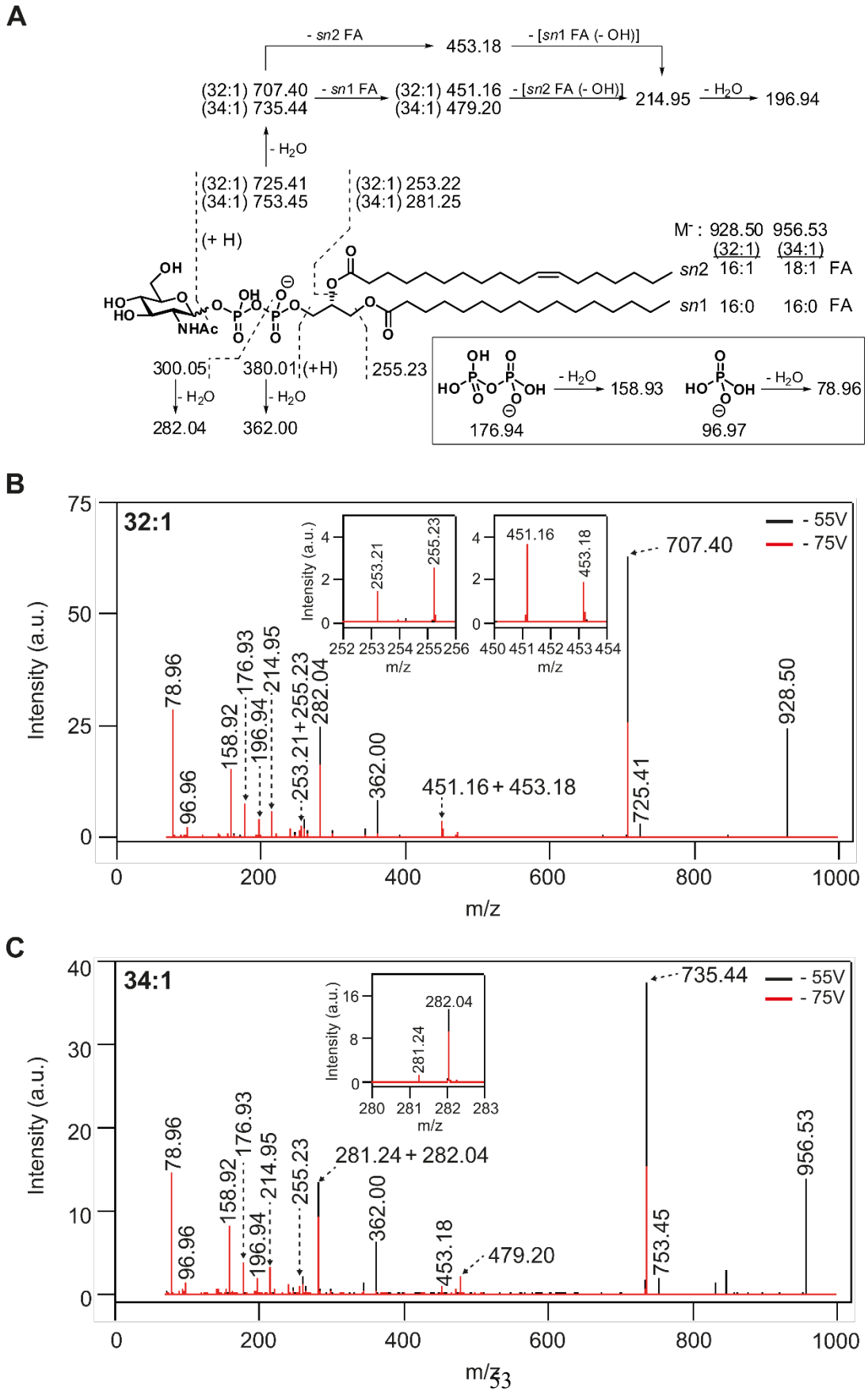
A
- sn2 FA
453.18
- [sn1 FA (- OH)]
(32:1) 707.40
(34:1) 735.44
- sn1 FA
(32:1) 451.16
(34:1) 479.20
- [sn2 FA (- OH)]
214.95
- H2O
196.94
- H2O
(32:1) 725.41
(34:1) 753.45
(32:1) 253.22
(34:1) 281.25
(+ H)
M- : 928.50 956.53
(32:1) (34:1)
sn2 16:1 18:1 FA
sn1 16:0 16:0 FA
300.05
380.01 (+H)
255.23
- H2O
282.04
362.00
176.94
158.93
96.97
78.96
B
32:1
- 55V
- 75V
707.40
928.50
725.41
451.16 + 453.18
362.00
253.21 + 255.23
282.04
Intensity (a.u.)
m/z
C
34:1
735.44
956.53
753.45
281.24 + 282.04
362.00
453.18
479.20
255.23
214.95
176.93
158.92
196.94
96.96
78.96

858

859 **Fig. 8** The chemical structures of DAG-PP-GlcNAc species are deduced from MS fragmentation
860 analysis. (A) Proposed fragmentation pattern with mass assignments of 32:1 and 34:1 DAG-PP-
861 GlcNAc species. (B and C) MS/MS spectra of (B) 32:1 and (C) 34:1 DAG-PP-GlcNAc species at
862 indicated collision energies. Spectrum at high collision energy (-75 V, red) is overlaid on top of
863 that at low collision energy (-55 V, black).
864